The Pennsylvania State University

The Graduate School

College of Engineering

ADAPTIVE DUAL CONTROL OF THE GLUCOSE REGULATORY SYSTEM IN PEOPLE WITH TYPE-1 DIABETES

An *in silico* experiment

A Thesis in

Mechanical Engineering

by

Kenneth A. Freeman

Submitted in Partial Fulfillment

of the Requirements

for the Degree of

Master of Science

August 2011

The thesis of Kenneth A. Freeman was reviewed and approved* by the following:

Qian Wang
Associate Professor of Mechanical Engineering
Faculty Advisor

Alok Sinha
Professor of Mechanical Engineering

Karen Thole
Professor of Mechanical Engineering
Department Head of Mechanical and Nuclear Engineering

*Signatures are on file in the Graduate School.

Abstract

A linear discrete time-varying model utilizing recursive parameter estimation coupled with an adaptive dual controller is presented for real-time modeling and control of the compromised glucose regulatory system in patients with type-1 diabetes mellitus. The performance of the proposed adaptive dual control for insulin delivery is evaluated via simulations using various performance indices widely adopted in existing literature. Compared to the clinical data (which include clinical measurement of glucose level, clinically-administered insulin delivery, and carbohydrate intake) collected from several patients over 72 hours, the simulation results show that the adaptive dual controllers developed in this thesis provide lower occurrence of hyperglycemia and hypoglycemia.

In simulations, a virtual patient in the form of a linear time-varying input-output model was built based on clinical data using Kalman-filter based recursive parameter estimation. This virtual patient is then used in the simulations to evaluate the proposed adaptive dual controller for insulin delivery. The clinical data include measurement of glucose level, estimated carbohydrate intake and insulin delivery rate for five patients over 72 hours in 5-minutes intervals. Due to temporary interruptions in the data, the longest stretch of uninterrupted data was used, of which 49 hours was the minimum. Each of the patients was diagnosed with type-1 diabetes and under continuous subcutaneous insulin infusion plus bolus treatment. The virtual patient model takes into account the absorption and transport time delays existed in the subcutaneous insulin injection and carbohydrate intake in its design of the finite impulse filters for the system inputs. In evaluation of the virtual patient model, model correlation coefficients which are generated between half-

hour future blood glucose prediction and clinical data glucose measurement, ranged from 0.84 to 0.96, showing sufficient model accuracy.

Based on Kalman-filter estimation of system parameters from the virtual patient (the algorithm itself does not depend on the model of the virtual patient, and hence can be applied to any simulation environments as well as real clinical environments), an adaptive dual controller is designed to determine the insulin injection based on the feedback information of the glucose measurement, together with the estimated carb intake.

The adaptive dual control algorithm minimizes two cost functions in the calculation of the control input in an attempt to cautiously track the target value while simultaneously providing persistent excitation required for accurate parameter estimation. Simulations show that the adaptive dual controller developed in this thesis has better control of type-1 diabetes with statistical significance when compared with the clinical treatment used during data acquisition. The results show that the adaptive approach based on real-time model estimation coupled with dual control could be a potentially very promising tool for closing the loop in blood glucose control in those with type-1 diabetes.

Compared to the conventional approaches based on compartmental models and non-adaptive control designs (either classical PID controllers or modern optimal control designs) in the current literature, the proposed empirical modeling based on online recursive parameter estimation, together with adaptive control design has several advantages. First, the modeling and control designs can be used for patients in a natural

living condition, with meal intake and exercises, noting the lack of a good meal model in the existing compartmental-model based control designs. Second, the proposed adaptive control approach provides the ability to track the time-varying behavior in a diabetic patient and react fast. Finally, the proposed framework allows easy extension to taking into account various factors that could affect patient's diabetic control such as exercises, stress levels, etc in the future study.

Table of Contents

List of Figures

List of Tables

List of Abbreviations

AP	Artificial Pancreas (or Artificial Endocrine Pancreas)
BG	Blood Glucose Concentration
BW	Body Weight
CHO	Carbohydrate
CGMS	Continuous Glucose Measurement System
CSII	Continuous Subcutaneous Insulin Infusion
DKA	Diabetic Ketoacidosis
ePID	External Physiological Insulin Delivery System
GRS	Glucose Regulatory System
GW2B	GlucoWatch G2 Biographer
HGH	Human Growth Hormone
IBW	Ideal Body Weight
IFG	Impaired Fasting Glucose
IGT	Impaired Glucose Tolerance
IIR	Insulin Infusion Rate
iPID	Implanted Physiological Insulin Delivery
ISO	International Organization for Standardization
IVGTT	Intravenous Glucose Tolerance Test
ip	Intraperitoneal
iv	Intravenous
LTI	Linear Time-Invariant

LTSS	Long-Term Sensor System
LTV	Linear Time-Variant
MPC	Model Predictive Control
NDDG	National Diabetes Data Group
OGTT	Oral Glucose Tolerance Test
PD	Proportional-Derivative
PDD2	Proportional-Derivative-2nd Derivative
PI	Proportional-Integral
PID	Proportional-Integral-Derivative
SMBG	Self-Monitoring of Blood Glucose
sc	Subcutaneous
std	Standard Deviation
T1DM	Type 1 Diabetes Mellitus
T2DM	Type 2 Diabetes Mellitus
WHO	World Health Organization

Acknowledgments

Foremost, I would like to thank my advisor Dr. Qian Wang for her guidance and advice during my work on this research project. Without her, this work would have not been completed and refined in such a timely manner. My thanks also extend to Dr. Jing Zhou and Dr. Peter Molenaar for their assistance, advice and support throughout the course of this work. They have been an invaluable resource. Additional thanks go out to the remaining members of our research group: Dr. Jan Ulbrecht, Dr. Mike Rovine, Dr. Carol Gold. Their ideas and advice have guided this work from the start.

This work is partially supported by CTSA Pilot project at the Pennsylvania State University. We, as a research group, are extremely thankful for the support this has provided.

Lastly, I would like to thank my family. My parents, Mr. Wayne and Mrs. Ginny Freeman, brother Mr. Michael Freeman and fiancée, Ms. Nicole McCoy, for their love support, and enduring devotion through these last few years.

Kenneth A. Freeman

August 2011

Pennsylvania State University, University Park, PA

Chapter 1: Diabetes Mellitus: An Introduction

1.1 Overview

Type-1 diabetes mellitus is a disease of the glucose regulatory system (GRS) in which, the blood glucose concentration is completely uncoupled from pancreatic insulin secretion. In type-2 diabetes, either the pancreas does not produce insulin in sufficient quantity, or the insulin produced is not effectively utilized by insulin sensitive tissues (impaired insulin action). Several pathological processes have been linked to the development of diabetes mellitus, including: autoimmune destruction of the beta cell, naturally increasing insulin resistance, and naturally decreasing insulin secretion [30]. Diabetes mellitus is diagnosed by either fasting hyperglycemia or by elevated glucose levels during an oral glucose tolerance test (OGTT) [30].

Until the National Diabetes Data Group (NDDG) published their classification system [66] in 1979, there was "no general accepted systematic categorization" for diabetes mellitus [30]. The World Health Organization (WHO) expert committee on diabetes and the WHO study group on diabetes later backed the findings of the NDDG system. Revisions on the initial classifications of diabetes later came from the Expert Committee on the Diagnosis and Classification of Diabetes Mellitus [31, 32]. These organizations defined a few types of diabetes. The most common two have been aptly named type 1 and type 2, while gestational diabetes mellitus and prediabetes are less publicly discussed forms [16]. All forms of diabetes relate to the patients inability to naturally control blood glucose [17, 30].

Type 1 diabetes mellitus (T1DM), previously called Insulin-Dependent Diabetes Mellitus (IDDM) or juvenile onset diabetes mellitus, is an autoimmune disorder and results in the destruction of pancreatic beta cells by the subject's immune system. These beta cells are the only natural source of the hormone insulin which is crucial in regulating blood glucose [30, 31]. Type 1 diabetes is common in children and young adults but has been known to onset at any age. Type 1 diabetes accounts for between five and ten percent of diagnosed cases. Risk factors for type 1 diabetes include autoimmunity, genetic and environmental [17, 30].

Type 2 diabetes mellitus (T2DM), previously called non-insulin-dependent diabetes mellitus (NIDDM) or adult onset diabetes, is characterized by a lack of insulin secretion and/or an increased resistance to the action of insulin (insulin resistance: IR). It is often undiagnosed until serious long term complications arise [30]. Type 2 diabetes mellitus makes up ninety to ninety-five percent of all diagnosed cases. During the onset of type 2 diabetes, the action of insulin is reduced (increased insulin resistance). This requires the pancreas to secrete more insulin, eventually reducing the pancreases ability to produce it [17].

Gestational Diabetes occurs in some women during pregnancy and requires treatment to void infantile complications. Obesity and genetics are the main risk factors. Women with gestational diabetes may develop permanent diabetes, usually being type 2. This occurs

immediately after pregnancy for between five to ten percent of women and for fifty percent of women in ten years [16, 17].

Prediabetes is a condition where unusual blood glucose levels are present but are not significant enough to diagnose diabetes. People with prediabetes are at an increased risk of developing T2DM. Impaired fasting glucose (IFG) and impaired glucose tolerance (IGT) are indicators of prediabetes [17]. IFG occurs when the blood glucose is between 100-125 mg/dl after an overnight fast. IGT occurs when the blood glucose level is between 140-199 mg/dl after a two hour glucose tolerance test [31]. For the years 1984-1994, of all adults in the United States, 33.8% had IFG, 15.4% had IGT and 40.1% had prediabetes (IGT, IFT or Both) [17]. The progression from prediabetes to diabetes is not guaranteed. Losing weight and increasing physical activity has been shown to reduce blood glucose levels to normal [17].

People with type 1 diabetes require insulin deliveries from outside sources due to the lack of β-cell population. Type-2 diabetics may require deliveries to supplement their insufficient production, inadequate utilization, or both [17]. Decreasing body weight, following a specific diet, exercising, and taking oral medications all can reduce the need for exogenous insulin. Many methods and devices are available for insulin delivery. The deliveries are accomplished using either an insulin pump or via direct injection. In both cases insulin is deposited into the subcutaneous tissue. Of those diagnosed with diabetes (types 1 and 2) between 2004 and 2006 in the United States, fourteen percent take insulin

only, thirteen percent take both insulin and oral medication, fifty-seven percent take oral medication only and 16 percent take no medication [17].

Currently, treatment of diabetes is a process which requires measuring the blood glucose regularly and deciding on appropriate bolus delivery amount around meal time. This decision is routinely (and intuitively) made based on current blood glucose, past blood glucose, past insulin delivery, past carbohydrate intake and forecasted carbohydrate intake. Some basic equations have been developed for calculating an appropriate dosage of insulin from a known meal size (see the 1500 and 1700 Rules [26]). These equations are general and must be modified to the individual patient.

The main affect of the disease is hyperglycemia; which results in chronic health problems. However, hypoglycemia is a major side effect of treatment, specifically over-treatment [25]. Hypoglycemia has acute effects and poses more of an immediate danger to the body.

Complications from hyperglycemia include heart disease, stroke, blindness (retinopathy) high blood pressure (hypertension), kidney disease (nephropathy), nervous system disease (neuropathy), amputations, dental/gum disease (gingivitis), sexual dysfunction, and complications during pregnancy [17, 30]. These complications have been related to the degree of "uncontrolled" blood glucose over time, most being chronic conditions [17]. Retinopathy, nephropathy and peripheral neuropathy are the most common [17, 30].

Polyuria (frequent urination), polydipsia (frequent drinking/thirst), polyphagia (frequent eating/hunger), and weight-loss are common symptoms of hyperglycemia [30].

The vast majority of hypoglycemic episodes in patients with type 1 diabetes mellitus (T1DM) result from the over administration of insulin, so-called iatrogenic hypoglycemia [25]. Treatment can push the blood glucose concentration low enough that cognitive impairment, blurred vision, unconsciousness, organ failure, coma, and death have been known to result. Hypoglycemia has been defined as a blood glucose concentration less than 60 mg/dl (with some restrictions, which will be defined later) [41, 25], and severe hypoglycemia less than 30 mg/dl [94].

In 2007, the direct medical expenses related to diabetes were estimated to reach $116 billion. Indirect expenses such as disability payments, work loss, and premature death were estimated at $58 billion. This totals to $174 billion in 2007 alone [17]. With these large figures, it is no wonder that in recent years there has been such a vast amount of research relating to achieving closed-loop control and finding a permanent cure.

1.2 The Biology behind the Disease

Extracting usable energy from chemical compounds, stored primarily in the bonds of the structure, is known as metabolism [55]. Glucose is the primary fuel used in metabolism in the human body. The pancreatic hormones insulin and glucagon are the tools the body uses in the regulation of glucose metabolism. These two hormones have opposite effects on the blood glucose concentration and thus have opposite triggers. Other hormones,

such as: epinephrine, cortisol and the human growth hormone (HGH) have also been shown to have minor influences in regulation [25].

In normal humans, when the blood glucose concentration is low, insulin concentration drops (there-by reducing insulin dependent glucose utilization, see below) and α-cells in the pancreas produce glucagon. The glucagon triggers the liver into producing glucose (hepatic glucose production or endogenous glucose production). This glucose is made from glycogen (stored in the liver) and glucagon. This glucose is then secreted back into the blood stream, raising the blood glucose concentration [55]. When the blood glucose is very low, elevated levels of the hormones epinephrine, cortisol, and HGH help stimulate hepatic glucose production and slow insulin dependent glucose utilization [25]. Elevated blood glucose concentrations cause the α-cells stop making glucagon and the β-cells start producing insulin. In most cells, insulin is required for glucose to pass through the cell membrane. When insulin receptors are filled, glucose transporters (specifically GLUT4) aid glucose uptake into skeletal muscle and adipose tissue (the main consumers of glucose) [90]. GLUT4 transporters, and thus glucose utilization, have also recently been shown to be activated by exercise [36, 38, and 90]. The liver is also a consumer of glucose. Hepatic glucose uptake allows the liver to act as described above, as a counter regulatory (prevent hypoglycemia) agent. Renal clearance of glucose to the urine is another natural regulatory measure. Glucose uptake lowers the blood glucose concentration completing the closed loop system. The major parts of a healthy glucose regulatory system (GRS) are diagramed in Figure 1.1.

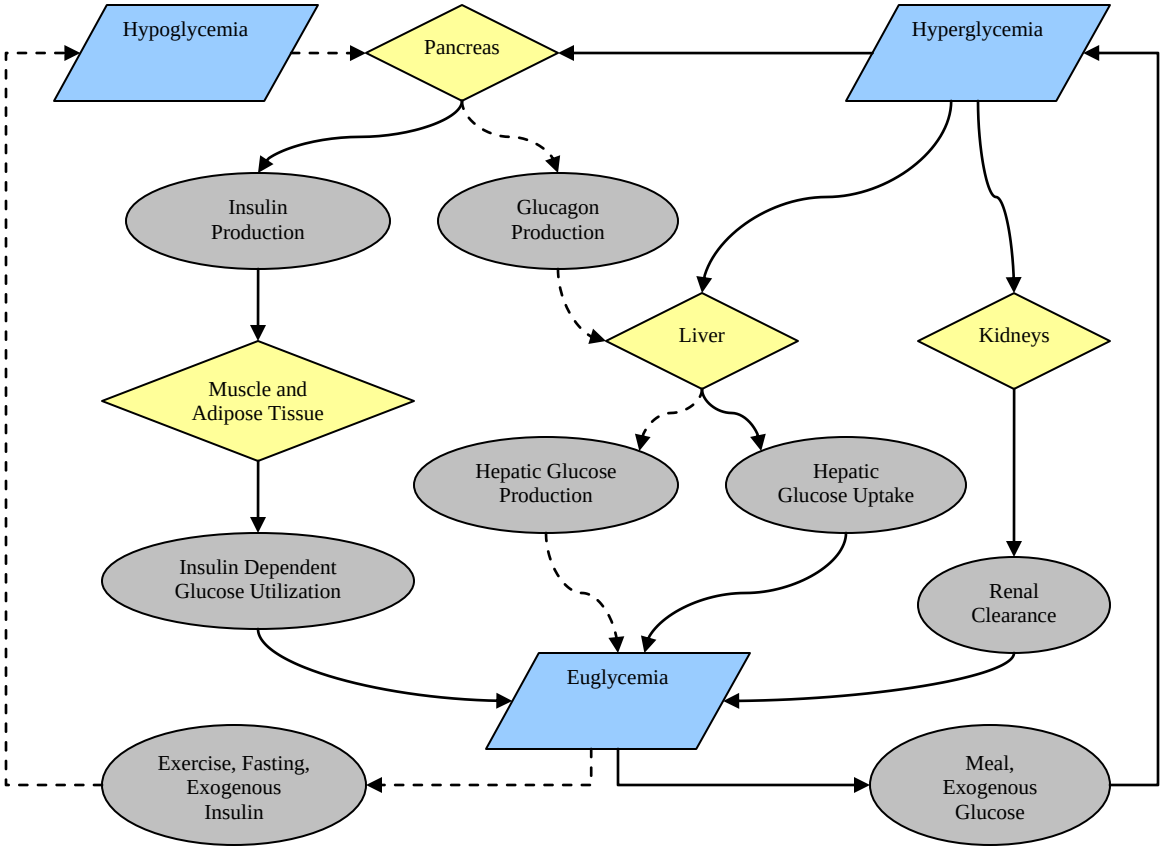

Figure 1.1: Diagram of the main functions in the glucose regulatory system

In diabetic people, the pancreas does not produce insulin (or enough insulin) and/or the action of insulin (glucose transportation into cells) is compromised (insulin resistance) [30]. This results in partial or complete dysfunction in the glucose regulatory system (GRS), ultimately manifesting itself as hyperglycemia. Additionally, counter regulatory functions (such as glucagon and epinephrine secretion) have also been shown to be compromised in people with type 1 diabetes mellitus (T1DM) [25]. The counter regulatory functions in those with type-2 diabetes mellitus (T2DM) has been shown to degrade with time [25].

Many outside influences make the regulation of glucose a difficult task. Natural disturbances, in the form of digestion forced glucose increases, occur primarily after meals and snacks (postprandial hyperglycemia). During treatment of diabetes, unnatural disturbances frequently occur in the form of exogenous insulin and glucose injections and intake. These events make the blood glucose trajectory rather time variant. Iatrogenic hypoglycemia is the major obstacle in achieving euglycemia in diabetic patients and makes control a non-trivial task [25].

1.3 Blood Glucose Measurement

The measurement of the blood glucose concentration started to gain technical attention in the middle of the last century, as noted by [48, 93]. Ever since these times, blood glucose measurement has been an essential part of the treatment of diabetes. Sensor accuracy is, of course, very important in this specific case due to the possibility of insulin over-dosage. Originally, many traditional statistical measures were used to characterize accuracy of glucose measurement including linear regression, percent deviation, and standard deviation. These statistics, while sufficient for most applications, have specific problems in accurately describing glucose sensor performance (these problems are further discussed in [18]). In 1987, Clarke et al devised an error grid analysis which rates the difference of the reference value and system generated value into five zones (A-E, A being good, E being not good). Although the error grid analysis is not a perfect statistic [24], it has become widely reported in literature [27, 64, and 92].

In the case of self monitoring of blood glucose (SMBG), measurement inaccuracy encompasses both inherent sensor inaccuracy and human misinterpretation. For closed-loop systems, the human impact is avoided.

'Finger-stick' devices have become commonplace in the management of diabetes. There are a plethora of devices on the market today, most being relatively cheap. For this reason, a review of all the devices on the market will not be given. However, reviewing accuracy of these meters is important. According to [67], there is no universal standard of measurement error for "finger-stick" monitors. However, the International Organization for Standardization (ISO) 15197 is widely accepted. This states that for blood glucose levels less than 75 mg/dl, meters should report values less than 15 mg/dl from the reference value. For blood glucose levels above 75 mg/dl, the meter should report values no more than 20% from the reference value. For obvious reasons, it has been suggested that the error tolerance over the entire range of glucose values be changed to ±5 mg/dl from the reference value [67].

The first commercial continuous blood glucose meter came on the market in 1999. The Continuous Glucose Monitoring System (CGMS; Medtronic MiniMed, Northridge CA, USA) uses a hydrogen peroxide-based enzyme electrode to accomplish the sensing. Samples are taken from the subcutaneous (sc) tissue. Sampling at ten seconds intervals, the meter filters the data and stores a reading every five minutes, with data stored for a maximum of three days [41]. The system has an inherent time-delay of two and a half minutes [28]. Calibration is recommended four times per day via comparison with self-

monitoring of blood glucose (SMBG) and requires another commercially available meter. A newer, more accurate 'Gold' version was realized in 2002 [28].

Many studies have focused on this initial monitoring system [62, 63] (most of which are summarized in [41]). The studies claim a CGMS to SMBG correlation of 0.85, a mean absolute deviation of 15% with 42% of readings within 15 mg/dl of the reference [41, 28]. Sensor failure rate was recorded at 28%. Over estimation of hypoglycemic and hyperglycemic episodes were recorded with reproducibility also in question [41]. Though not without its problems, the CGMS led the continuous blood glucose monitors onto the market.

The long term sensor system (LTSS; Medtronic MiniMed, Northridge CA, USA) uses their long term glucose sensor to measure blood glucose intravenously (iv). It has been reported that >95% of LTSS reported measurements lie within zones A and B of the Clarke error grid. Additionally, the LTSS has been shown to provide reliable readings for 14 months [75].

The GlucoWatch G2 Biographer (Cygnus, Redwood City, CA) received FDA approval in 2002 as a temporary (thirteen hour maximum) continuous monitoring device. It operates without puncturing the skin by electrically pulling fluids through the skin and produces a measurement each ten minutes [32]. This method, while convenient, yields a glucose value that has a mean seventeen-and-a-half minute time delay compared to a venous measurement. The meter has been shown to be less accurate than the CGMS with 31%

of reading within 15 mg/dl of the reference and a false hypoglycemic alarm rate of 51% [28]. The GlucoWatch G2 Biographer is a convenient alternative to the CGMS, however, due to the longer measurement delay and higher measurement error, it is not as useful to those focused on achieving closed-loop (CL) control.

In 2004, Guardian Continuous Monitoring-System (GCMS; Medtronic MiniMed, Northridge CA, USA) was realized. It acquires interstitial glucose readings every 5 minutes after an initial calibration and can provide the user with alerts for both low and high glucose levels. Sensor replacement intervals were not stated. According to MiniMed, the sensor has a mean absolute difference (from reference values) of 19.7% with 61.7% and 34.4% were in zones A and B respectively of the Clarke error grid [64].

The Free Style Navigator (Abbott Diabetes Care, Alameda, CA) was approved by the FDA for continuous glucose monitoring over the course of five days. The system requires a ten hour start up period with calibration accomplished internally and provides an interstitial glucose measurement every minute [92]. The sensor has been shown to be rather accurate over the five day period with 81.7% and 16.7% in zones A and B of the Clarke error grid [92].

The DexCom Seven STS continuous glucose monitor appeared on the market in 2007 [CM]. A revised Seven+ version has recently been released [27]. DexCom reports that the monitor can accurately measure subcutaneous glucose for a period of seven days with calibrations occurring every twelve hours. It was reported that 96% of all measurements

lie within zones A and B of the Clarke error grid [27]. Other reports have shown this sensor to have an operational life on the order of three months [75].

Chapter 2: Literature Review on GRS Models and Closed-loop Control Prototypes

This chapter gives a short review on mathematical models and closed-loop controllers for the glucose regulatory system (GRS). More extensive reviews can be found in [41, 42, 57, and 85].

2.1 GRS Models

GRS models have been developed for many purposes. Initially they were developed to aid in understanding the inherent dynamics in normal (non-diabetic) animals and people. Models eventually expanded into the realm of diabetic subjects where, among other things, endogenous insulin production is compromised. In recent years, new models have focused on complementing a potential artificial pancreas (AP), specifically on selecting appropriate insulin injection amounts.

It is important to note that most GRS models have a compartmental structure which characterizes the flow of material (glucose, insulin, etc) through different tissues and organs. GRS models have been traditionally classified into two general categories: minimal (simple) and comprehensive (complex) [19]. Simply put, minimal models attempt to simulate the most important governing relationships with, as the name suggested, the minimum amount of terms. More aggressive definitions have stated all parameters should be *a priori* identifiable. Either way, these models are friendly in terms of mathematical tractability. Comprehensive models are focused on modeling everything

of importance in order to achieve the desired correlation, without regard to mathematical tractability, model reproducibility and parameter identifiably. This categorization will be maintained within this work.

Assessing the quality of each model can be accomplished by analyzing its realism and robustness [19]. Validation of realism is done through correlating model predictions and parameters to clinical measurements. Determining robustness is done is much the same way, but occurs under a variety of operating conditions. A robust GRS model should be able to accurately simulate the dynamics during conditions ranging from fasting to meals and exercise.

2.1.1 Comprehensive Models

In 1975, Carson and Cramp [15] developed one of the first comprehensive models. Its multi-compartment nonlinear structure was developed to include explicit relations of the physiology known at that time. The model consists of six compartments: blood glucose, liver glucose-6-phosphate, liver glycogen, blood insulin, blood glucagon, and blood adrenalin (epinephrine). This model is a great example of the comprehensive type due to the vast amount of information the creators tried to simulate.

In 1981, Cobelli and his colleagues [21] introduced a new concept of having multiple compartments for one compound. Both glucose and glucagon subsystems have one compartment each. However, the insulin subsystem has a total of five compartments corresponding to the pancreas, liver, portal plasma, plasma and interstitial fluid. Like most GRS models, the model developed by Cobelli et al uses mass balance equations to

describe the flow of material. In this case, glucose, insulin and glucagon are analyzed. Similar to many other GRS models, determining some of the model parameters can be difficult due to the inability of observing them. Model performance was based on comparison to clinical data obtained during intravenous glucose tolerance tests (IVGTT) performed on five separate human subjects. Correlation was good, but data was limited to 90 minutes making prediction past that mark extraneous. Insulin-dependent glucose utilization is important within the context of this thesis. Figure 2.1 shows both insulin-dependent glucose utilization and the model correlation.

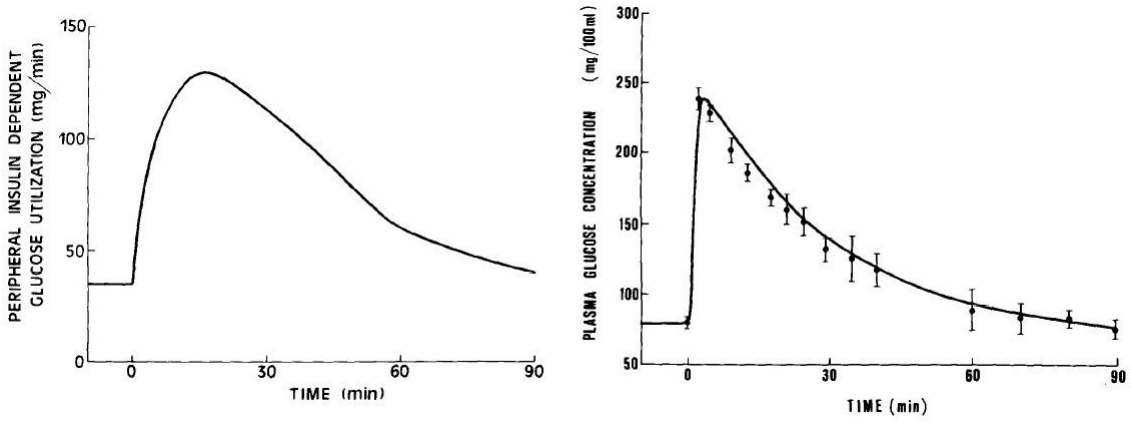

Figure 2.1: Modeled Insulin-Dependent Glucose Utilization (Left) and Comparison of model prediction to clinical data following an IVGTT in a non-diabetic human (Right), adopted from [21]

Lehmann and Deutsch published a model in 1992 [54]. The primary goal of this model was to educate patients and medical professionals on how to effectively control type-1 diabetes. This is achieved via showcasing the effects of proper and improper insulin dosing on blood glucose. The model consists of a single glucose compartment, representing the blood plasma, and two insulin compartments. The insulin has been

separated into plasma and 'active' insulin. Glucose enters its single compartment by way of a time-delayed gastric absorption and hepatic production. Glucose exits the compartment through insulin dependent utilization (muscle and adipose tissues), independent utilization (central nervous system and red blood cells (RBC)), hepatic intake, and renal secretion to the urine [54]. Plasma insulin is governed by subcutaneous injection and hepatic degradation. Active insulin is related to plasma insulin through first order dynamics and is responsible for glycemic control. The renal secretion of glucose is an important feature of this model above the previously described. It is modeled in a piecewise nature: zero secretion below a specified blood glucose threshold and linear with blood glucose above that threshold. The slope of the linear portion represents the creatinine clearance (glomerular filtration) rate [54].

The model by Hovorka et al presented in [44, 45] is the state of the art in terms of the structure of the glucose regulatory system. It is a time-varying, non-linear, multi-compartment model containing multi-compartment subsystems which describe subcutaneous insulin absorption/action and glucose absorption from the gut. This model is especially important due to its contribution into recent attempts at the Artificial Pancreas (AP). The model is given by Equation 2-1 through Equation 2-9.

$$\dot{Q}_1 = -\left[\frac{F_{01}^c}{V_G G(t)} + x_1(t)\right] Q_1(t) + k_{12} Q_2(t) - F_R \ldots$$
$$\ldots + U_G(t) + EGP_0\left[1 - x_3(t)\right] \qquad \textbf{Equation 2-1}$$

$$\dot{Q}_2 = x_1(t) Q_1(t) - \left[k_{12} + x_2(t)\right] Q_2(t) \qquad \textbf{Equation 2-2}$$

$$G(t) = Q_1(t)/V_G \qquad \textbf{Equation 2-3}$$

$$U_G(t) = D_G A_G t e^{-t/t_{\max,G}}$$ **Equation 2-4**

$$\dot{S}_1 = u(t) - \frac{S_1(t)}{t_{\max,I}}$$ **Equation 2-5**

$$\dot{S}_2 = \frac{S_1(t)}{t_{\max,I}} - U_I(t)$$ **Equation 2-6**

$$U_I(t) = \frac{S_2(t)}{t_{\max,I}}$$ **Equation 2-7**

$$I = \frac{U_I(t)}{V_I} - k_e I(t)$$ **Equation 2-8**

$$\sum_{i=1}^{3} x_i = k_{ai} x_i(t) k_{bi} I(t)$$ **Equation 2-9**

where, Q_1 and Q_2 represent the blood glucose mass in the accessible and non-accessible compartment respectively, V_G and V_I are the distribution volumes of the accessible glucose and insulin compartments respectively, G is the measurable blood glucose, EGP_0 is the endogenous glucose production, F_{01}^c is the non-insulin dependent glucose utilization, F_R is the renal glucose clearance, U_G is a two compartment chain of glucose absorption from the gut, U_I is the insulin absorption rate, $t_{max,G}$ and $t_{max,I}$ are the times of maximum absorption rates for the glucose and insulin respectively, and $k_{12,}$ k_e, k_{a1}, k_{a2}, k_{a3} are transfer rate constants.

Many other comprehensive models can be found in [2, 29, 35, 39, 55, 58, 59, 78, 82, 89, 91, the review paper 57] and references therein.

2.1.2 The Minimal Model and Its Variants

The *minimal model* was first developed by Bergman et al [9] in 1979 in their attempt to make measuring insulin sensitivity less invasive then previous methods. Since then, it has become the most widely studied model. Many revisions have been published afterwards [10, 12, 22, 23]. The minimal model is given by Equation 2-10 and Equation 2-11.

$$\dot{G} = (p_1 - X(t))G(t) + p_4 \qquad \textbf{Equation 2-10}$$

$$\dot{X} = p_2 X(t) + p_3 I(t) \qquad \textbf{Equation 2-11}$$

where G is the blood glucose concentration, I is the blood insulin concentration, X is a variable proportional to the blood insulin concentration, p_1 and p_2 are material transfer rates, p_3 is a conversion factor and p_4 is the net expected hepatic glucose balance.

In [9], to evaluate the minimal model, a series of Intravenous Glucose Tolerance Tests (IVGTT) were conducted on a set of five non-diabetic canines. Glucose and insulin concentrations were recorded every minute for one hour following the injection of three different quantities of glucose: 100, 200 and 300 in units of milligrams per kilogram of body weight (mg/kg). The data was then fed into seven different and relatively simple dynamic models. Each model was systematically scored on its ability to predict the blood glucose concentration based on estimated model coefficients. The 'best' model was selected on its ability to predict blood glucose concentration for each of the three injection amounts (see Figure 2.2). Lines indicate model estimates, circles are data points. The smaller of the two lines is plotted on a second axis and represents the volume of insulin in the remote compartment.

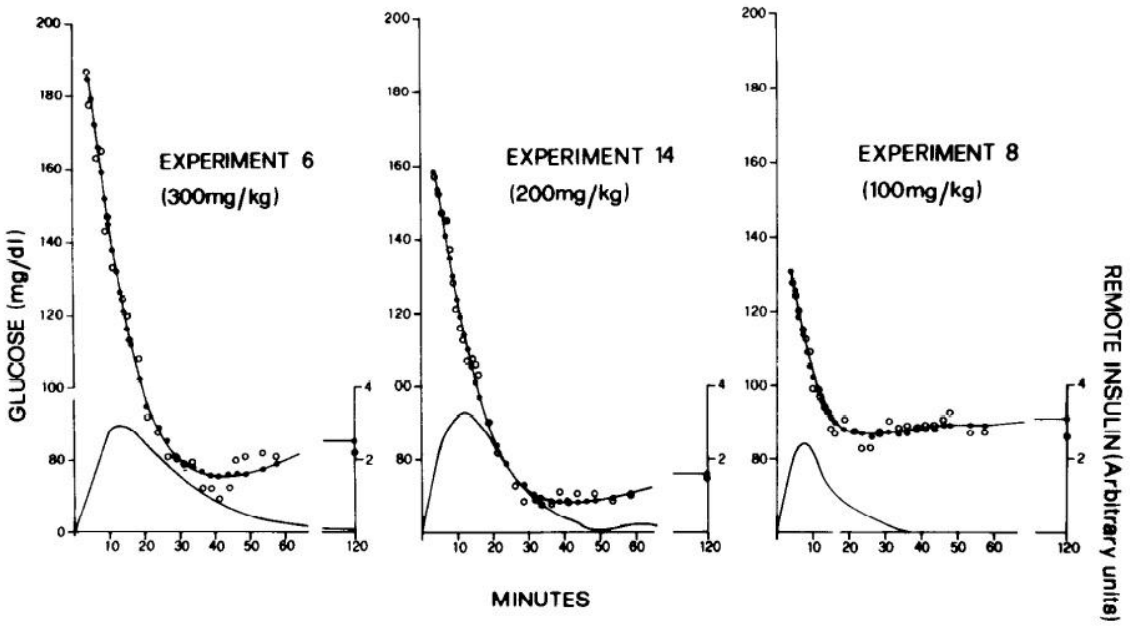

Figure 2.2: Prediction of blood glucose concentration and simulated insulin volume in the remote compartment following IVGTT in canines (figure adopted from [9])

In [9], the insulin sensitivity index (S_I) is introduced as a ratio of model parameters, given by Equation 2-12. This is a measure of how much the glucose concentration will decrease based on a specified amount of insulin concentration. Similarly, the glucose effectiveness (S_G) is defined and given by Equation 2-13.

$$S_I = -p_3 / p_2 \qquad \textbf{Equation 2-12}$$

$$S_G = p_1 \qquad \textbf{Equation 2-13}$$

A three compartment version of the minimal model was published in 1999 by Cobelli et al [20] in an effort to better model insulin sensitivity (S_I) and the glucose effectiveness index (S_G). Data had shown these values to be underestimated and over estimated respectively [20]. The main modification by Cobelli et al to the minimal model is the addition of a non-accessible glucose compartment. The non-accessible nature of the new

compartment forced Bayesian parameter estimation to be used in modeling instead of their preferred clinical measurement approach. The revised model is given by Equation 2-14 through Equation 2-16.

$$\dot{Q}_1(t) = -\left[p_1 + k_{21} + X(t)\right]Q_1(t) + k_{12}Q_2(t) + p_1 Q_{1b} \quad \textbf{Equation 2-14}$$

$$\dot{Q}_2(t) = k_{21}Q_1(t) - k_{12}Q_2(t) \quad \textbf{Equation 2-15}$$

$$\dot{X}(t) = -p_2 X(t) + p_3[I(t) - I_b] \quad \textbf{Equation 2-16}$$

$$S_G = p_1 V_1 \quad \textbf{Equation 2-17}$$

$$S_I = \left(p_3 / p_2\right)V_1 \quad \textbf{Equation 2-18}$$

2.2 Closed Loop Control for T1DM

Traditionally, blood glucose concentration in patients with type-1 diabetes mellitus (T1DM) is controlled by providing the body with exogenous insulin in the form of either bolus only or boluses combined with basal insulin. The latter is frequently referred to as continuous subcutaneous insulin infusion (CSII) and is accomplished with the assistance of an insulin pump.

In either case, the dose of a preprandial insulin bolus is routinely calculated through the estimation of the carbohydrate (CHO) content of the anticipated meal [26] and a pre-meal blood glucose measurement. Both treatment methods mentioned above employ subcutaneous (sc) blood glucose (SMBG) testing at regular intervals to detect and avoid deviations from euglycemia through either additional insulin injections or food consumption.

Various closed-loop control algorithms have been implemented on various models and in clinical settings. These include classic controllers, most notably the proportional-integral-derivative (PID) (and its variants) and the linear model predictive controller (MPC) [49]. Other control schemes such as non-linear MPC [44], robust H_∞, and sliding mode control have also been implemented [50].

The insulin infusion rate (IIR) corresponding to the PID controller is given by (Equation 2-19), where BG(t) is the measured blood glucose at time 't' [41]. Controller gains K_P, K_I, K_P and K_C usually are constants tuned offline using a validated numerical model of the system under control. G_t is the target value of the blood glucose and can be selected.

$$IIR(t) = K_P(BG(t) - BG_t) + \ldots$$
$$\ldots K_I \int (BG(t) - G_t)dt + K_D \frac{dBG(t)}{dt} + K_C$$

Equation 2-19

The insulin infusion rate determined by MPC results from minimizing a cost function over some finite horizon. For a general linear time variant (LTV) system characterized by A(t) and B(t), Equation 2-20 represents a quadratic cost function to be minimized with represent to the input 'u', where the matrices Q and R represent the weight on the state(s) and input(s) respectively.

$$J = \min_u \int [x^T(t)Qx(t) + u^T(t)Ru(t) + 2x^T(t)Nu(t)]dt$$

$$s.t. \begin{cases} \dot{x}(t) = A(t)x(t) + B(t)u(t) \\ x(t0) = x0 \end{cases}$$

Equation 2-20

In addition to the various controllers, there are a few interfacing options when connecting a closed loop (CL) system to a patient [41]. The variety of options related to how the blood glucose in measured and how the insulin is injected. There are two basic

measuring paradigms. The first option is to subcutaneously (sc) measure the blood glucose concentration. This method, however useful, is fundamentally flawed, because the glucose concentration in the subcutaneous tissue is not the blood glucose concentration [72]. It has been shown to have a time delay of about 25 minutes [41]. The second option is to measure it intravenously (iv). This yields a faster measurement but has issues with implanting the sensor, infection, etc.

There are three major schemes of insulin delivery. The first is to subcutaneously deliver insulin. This is currently the most widely used method as both insulin pens and pumps fit into this category. It has the advantage in that there are over 200,000 wearable insulin pump users [46, 69]. However, this method has a large time delay associated with absorption [41] and could potentially lead to controller instability. The second option is to delivery insulin intravenously and is the closest to duplicating nature. Delivering insulin intraperitoneal (ip) tissue is the third option. There is a slightly less absorption time delay when compared with the sc route [41] but is still greater than an iv injection [52].

When combined in an abbreviated form, these sensing/delivery routes make an efficient categorization of closed loop systems. Examples are a subcutaneous sensor combined with a subcutaneous delivery method, appropriately abbreviated sc-sc. Likewise, there are numerous combinations, including: iv-iv, iv-ip, sc-iv, etc.

It must be mentioned that though a potential engineered AP might have the ability to adequately replace a defective pancreas, it would, by no means, be a cure for the disease. Presenting potential cures for diabetes is outside the scope of this thesis, but could come in the form of stem cell treatment, islet transplantation, islet encapsulation, or other methods [42].

2.3 Obstacles and Challenges to Closed Loop Control

Iatrogenic hypoglycemia is the major hurdle to overcome in order for closed-loop control to reach mainstream society, due to its acute and potentially deadly effects [12, 25, and 88]. The main cause is over-dosing insulin, something easily attainable through an insufficiently engineered system. The glucose regulatory system is a high-order, non-linear, time-variant, and population-variant system [44]. These facts make preventing hypoglycemia whilst treating hyperglycemia, especially during and after meals, a difficult task. This difficulty in system control is made evident by the variety of health problems which commonly result under the current CSII plus bolus treatment method [17].

At this point in time, research has not granted us with the ability to continuously and confidently measure blood glucose without frequent calibration and/or sensor replacement over the long term. All CGM devices currently approved by the FDA have an 'adjunct' labels, meaning the continuous measurements do not replace SMBG [42]. Until continuous glucose sensors become reliable, long lasting and receive a 'replacement' label from regulatory agencies, closed loop control will only occur in clinical settings. Additionally, the time lag between blood glucose and subcutaneous

tissue glucose is significant [88]. Time-delays could have a destabilizing effect on closed-loop systems. Many sensors (described in section 1.3 of this thesis) measure the glucose concentration in the interstitial fluid of the subcutaneous tissue and this time delay should be taken into consideration during control design to avoid possible complications.

While historically, modeling the glucose regulatory system has yielded insight into the inner-workings of the bio-physical system and laid the groundwork for several adequately performing controllers (see section 2.5), but it has not yet produced a universal closed-loop control solution to diabetes. In addition to the common themes of GRS modeling, such as: insulin sensitivity and effect, carbohydrate (CHO) (or food) sensitivity and effect, renal clearance, non-insulin dependent glucose utilization, etc, one also must take a step back and wonder how these common themes are affected by other biophysical conditions and mental states. Conditions such as stress [91], fatigue, sexual arousal and other hormone levels (epinephrine, cortisol, growth hormone, adiponectin, and resistin) [15, 25, 47 and 91], could potentially have a great impact on the governing biology. For example, modeling the effects and consequents of exercise in patients with T1DM has not yet reached mainstream engineering literature [12]. However, a few studies have been focused on the physiologic changes which occur during exercise. These changes more generally include an increase in glucose utilization, hepatic glucose production, blood flow and heart rate [1, 12]. From experiments in diabetic rats, exercise has shown to significantly increase short-term glucose uptake into skeletal muscle and

adipose tissues [36]. Similarly, a long-term increase in insulin sensitivity has been shown to result from exercise, in both acute and chronic forms [38].

2.4 Evaluating Quality of Control

There is no universal measure of controller performance for type-1 diabetes treatment and management [41]. Many methods have been suggested: A1C blood test [17], diurnal mean blood glucose concentration [81], preprandial BG, two-hour postprandial BG, morning glycosuria [80], number of hypoglycemic events [41, 81], the percentage of time spent within euglycemia [40, 41, 80], mean amplitude of glycemic excursions (MAGE) [81], the M-value [80], the J-index [94] and the control-variability grid [56]. Among them, the first several measures are quite self-explained. In the following, more details on MAGE, M-value and J-Index are given.

The mean amplitude of glycemic excursions (MAGE) statistic was developed by Service et al [81] in the early '70s. It is a measure of the amplitude of the glucose extrema. However, only extrema which are greater then one standard deviation of the daily blood glucose from the last extrema are used in the calculation of MAGE [81].

The M-value was designed in the mid 1960's as a method of more heavily weighting hypoglycemic events while still effectively measuring the overall control [80]. The M-value has historically been the most widely used measure of glucose control, especially within the clinical setting [94]. One downside to this statistic is the variability in which it can be calculated [94]. The general form is shown in Equation 2-21 below, where '*A*' and

'*B*' are constants. These constants were initially chosen to be 10 and 80 respectively; however these have been modified several times [91]. In this thesis, two M-values will be reported. The two most common forms: A=10 with B=80, and A=10 with B=120 produce aptly named M_{80} and M_{120} statistics, respectfully.

$$M = mean\left\{\left|A * \log\frac{BG(t)}{B}\right|^3\right\} \qquad \textbf{Equation 2-21}$$

In 1990, the J-Index was developed in an effort to create a more uniform reporting statistic for blood glucose control [94]. It addition to Equation 2-22, the author published a scale consisting of 4 levels of control shown in Table 2.1.

$$J = 0.001\left[mean(BG(t)) + std(BG(t)\right]^2 \qquad \textbf{Equation 2-22}$$

Quality of Control	J-Index
Ideal	$10 \leq J \leq 20$
Good	$20 < J \leq 30$
Poor	$30 < J \leq 40$
Lack of Control	$J > 40$

Table 2.1: Grading Scale for J-Index [94]

With the mean blood glucose value, percentage of time within euglycemia, the MAGE, M80, M120, J-Index, and the number of hypoglycemic events, one has enough information to rate and compare controllers and clinical treatment. All of these statistics will be reported within the context of this thesis.

2.5 Closed Loop Prototypes

Simulation studies have been widely used in the research for GRS, e.g, in [14], a proportional-derivative-2nd derivative (PDD2) controller was designed and implemented on the minimal model [9, 23] (with some modifications) during IVGTT for various glucose loads; in [68], a linear MPC is applied to a nonlinear 19th order model during an OGTT; in [60], a bolus plus PID algorithm was designed using the model by Hovorka et al; to name a few. Several closed-loop systems have been developed throughout the years with implementation limited to a supervised clinical setting. Clinical experiments are expensive and potentially dangerous which is why numerical controller simulation is popular. However, some controllers have been tested in a supervised clinical setting with success. A short summary of these prototypes is given below and readers can refer to [41, 42, and 85] and references therein for detailed information.

In 1974, Dr. Albisser published the first attempt at an artificial pancreas with clinical tests on six dogs [3] and three humans [4]. They developed and tested an iv-iv type monitor and control scheme with the capability of delivering both insulin and dextrose. The dextrose was used as an agent to prevent hypoglycemic events. In other experiment, the system was implemented without the dextrose infusion to test a more practical system [11]. Later modifications to the original system were tested again with similar results [51, 61]. Insulin injection, of the original system [3, 4], was determined in two different ways. The first uses a function of current glucose measurement 'G' (Equation 2-23). The second function has the same form as the first, but uses a forward blood glucose prediction 'G_P' calculated from the rate of change in BG (Equation 2-24 and Equation

2-25). Dextrose injection was determined using the same functional relationship using different parameter values (Equation 2-26) [3]. Results were universally positive and are shown in detail in [3, 4, 51, and 61].

$$R_I = \frac{1}{2} M_I \left[1 - \tanh\left(S_I (G - B_I)\right)\right] \quad \textbf{Equation 2-23}$$

$$R_I = \frac{1}{2} M_I \left[1 - \tanh\left(S_I (G_P - B_I)\right)\right] \quad \textbf{Equation 2-24}$$

$$G_P = G + K_1 \left(e^{A/K_2} - 1 \right) \quad \textbf{Equation 2-25}$$

$$R_D = \frac{1}{2} M_D \left[1 - \tanh\left(S_D (G - B_D)\right)\right] \quad \textbf{Equation 2-26}$$

The Glucose Controlled Insulin Infusion System (GCIIS: or Biostator TM), introduced in 1977, was the eventual result of the initial research by Dr Albisser. Its use was limited to clinical settings due to its size, need for constant supervision, and tendency for over treatment of insulin. The tendency to over infuse insulin was partially due to the fully closed-loop (lack of meal announcement) nature of the controller [41].

Dr. Shichiri headed the group responsible for the second prototype of an artificial endocrine pancreas (AP). This work eventually resulted in a small bedside version, the STG-22 (Nikkiso Co. Ltd, Tokyo, Japan) [41, 49]. The initial models were of the sc-iv type. The STG-22 is of the sc–sc type and uses a combination of unmodified short-acting insulin and an insulin analogue (Lispro) [41]. They have most recently explored the sc–ip method [41]. The latest device is claimed to effectively maintain euglycemia over seven days with no calibration and fourteen days with one calibration [37, 41]. The glucose sensors used in these controllers have either been a micro-dialysis type [37] or a

needle type [83, 84]. A simple non-adaptive PD controller was implemented for the device (K_I=0) and K_P, K_D and K_C are functions of the insulin in use (unmodified short-acting or lispro) [84].

In more recent years, several groups have been intensely involved in developing the artificial pancreas (AP), including Hovorka et al, Renard et al, Medtronic MiniMed and others. Hovorka and his colleagues have completed several clinical control experiments focusing on a sc–sc type system. They include both closed-loop control with meal announcement [13, 44] and semi-closed-loop [43] control. These studies employed MPC using the model noted in section 2.1.1 of this thesis. Medtronic MiniMed implemented an external physiologic insulin delivery system (ePID), in 2004, to work in conjunction with the simultaneously realized Guardian Continuous Monitoring System [64]. The ePID controller was designed to emulate the first and second phase response of the β-cell through the implementation of a PID algorithm [85-87]. Renard et al [74-77] focused on utilizing the long-term sensor system (LTSS, described in section 1.3 of this thesis) developed by Medtronic MiniMed (Northridge, CA, US) [74-77] in combination with their implantable physiological insulin delivery system (iPID) which delivers insulin into the intraperitoneal (ip) cavity. The system has been clinically tested using a standard PD control algorithm in the fully closed loop mode. With the clinical success of these newest prototypes, it seems that achieving long term closed loop control is becoming more feasible. However, sensor problems still exist and closed loop control has yet to be tested outside of a clinical setting.

Chapter 3: Simulated Dual Control

This chapter contains the technical details and methods used within this thesis. This includes: clinical data acquisition, modeling of the GRS for type-1 diabetes, and the adaptive dual control design algorithm.

3.1 Clinical Data Acquisition

The Institutional Review Board at the Pennsylvania State University approved the study. Blood glucose concentration, insulin delivery and meal intake were recorded in five type -1 diabetic subjects over three days during free-living conditions. In some cases, the recorded data was temporarily interrupted. Therefore, for this work, only the longest stretch of uninterrupted data was utilized. The general characteristics of subjects and the respective data sets are shown in Table 3.1.

#	Age (yr)	Sex	Weight (kg)	Height (cm)	Pump Used	Data Length
1	40	M	81	170	MiniMed 508	588
2	30	M	120	198	Animas 1250	780
3	64	M	84	179	Animas IR 1200	589
4	44	F	60	159	Animas IR 1200	816
5	33	F	104	170	Animas 1200	850

Table 3.1: Subject attributes and acquired data length

Insulin dosage was recorded by each insulin pump and downloaded afterwards. The insulin analogue, lispro, was used by all subjects. The Animas 1200 series pumps deliver

basal insulin in pulses every three minutes. The Medtronic MiniMed 508 pump delivers 0.1 units of insulin uniformly dispersed in order to meet the programmed insulin infusion rate (IIR). Bolus size and delivery time were controlled by the subject. Glucose concentrations were recorded every five minutes using the Medtronic MiniMed Continuous Glucose Monitoring System (CGMS: model MMT-7102) and were downloaded to a PC at the end of the collection period. The manufacturer's directions for use (insertion, calibration, etc) were followed.

Subjects reported all meals and snacks in the form of time-stamped digital photographs. One photograph was taken prior to each meal/snack and, if any food was not eaten, another was taken of the remaining portion. Intake was estimated from the digital photographs and/or food packaging by a dietitian at the General Clinical Research Center (GCRC) during a debriefing session with each subject. This method of estimation has been shown to be acceptable [53]. Food intake was then entered into Nutritionist Pro Version 4.0.1 (Axxya Systems), which provided the carbohydrate content of the meals.

Additionally, exercise and their associated times were logged by each subject. Subjects 2 and 4 reported no formal exercise. Subject 1 rode bicycle for 25 minutes on two separate occasions. Subject 3 exercised for 30 minutes on a treadmill. Subject 5 reported cleaning and two hours of yard work on separate occasions.

Once all of this information was recorded, the insulin injection and carbohydrate intake was then resolved into five minute intervals matching that of the glucose monitor, thus

creating a time-stamped value for each blood glucose, insulin injection and carbohydrate intake. The exercise that was recorded was not used within this work.

3.2 Data-Driven Linear Discrete Time-Varying Model

Many previous attempts at modeling the glucose regulatory system (GRS) have either focused on a specific event (IVGTT, sc insulin bolus, etc), or have had issues with the inherent structure of the model (*a priori*) or large uncertainty in parameter selection/estimation (*a posteriori*) [19]. The lack of knowledge about system parameters limits the available options in system identification [5].

Inter-subject variability factors such as weight, age, gender, physical fitness, and insulin resistance make customizing models a must. Additionally, intra-subject factors such as the dawn phenomenon, acute illness, circadian and diurnal rhythms force model adaptation to occur [42]. Due to these factors, a data-driven linear time-varying model was selected in this research to model the GRS. The adaptive nature of the model allows it to track data well [65].

The model consists of three autoregressive components: blood glucose (Equation 3-3), insulin delivery (Equation 3-4) and carbohydrate (CHO) intake (Equation 3-5). A time delay on both insulin delivery and carbohydrate intake is realized through a normalized finite impulse response (FIR) function F (see Equation 3-6 through Equation 3-7) [95] and is representative of the delay of subcutaneous insulin absorption [7, 41] and gastric absorption [54] respectively. The finite impulse response filter can be seen in Figure 3.1.

$$BG(k+1) = G(k+1) + \varepsilon(k) \qquad \textbf{Equation 3-1}$$

$$G(k+1) = \Phi[G(k)] + \mathrm{B}[I_f(k)] + \Gamma[C_f(k)] \qquad \textbf{Equation 3-2}$$

$$\Phi[G(k)] = \sum_{i=1}^{p} \phi_i(k) G(k-i) \qquad \textbf{Equation 3-3}$$

$$\mathrm{B}[I_f(k)] = \sum_{i=1}^{q} \beta_i(k) I_f(k-i) \qquad \textbf{Equation 3-4}$$

$$\Gamma[C_f(k)] = \sum_{i=1}^{r} \gamma_i(k) C_f(k-i) \qquad \textbf{Equation 3-5}$$

$$F(i) = \begin{cases} \frac{1}{3}\left(f(1) + f(2)\right) \Big/ \|F\| & i = 1 \\ \frac{1}{3}\left(f(i-1) + f(i) + f(i+1)\right) \Big/ \|F\| & i = 2:35 \\ \frac{1}{3}\left(f(35) + f(36)\right) \Big/ \|F\| & i = 36 \end{cases} \qquad \textbf{Equation 3-6}$$

$$f(i) = \begin{cases} 0 & i = 1:4 \\ \frac{1}{\sqrt{2\pi\sigma}} \exp\left(-\frac{(i-\mu)^2}{2\sigma^2} \right) & i = 5:36 \end{cases} \qquad \textbf{Equation 3-7}$$

$$I_f = IF \qquad \textbf{Equation 3-8}$$

$$C_f = CF \qquad \textbf{Equation 3-9}$$

where, *BG* is the measurement of blood glucose, *G* is the actual blood glucose, *C* is the carbohydrate (CHO) intake, *I* is the insulin injection, ε is the measurement error, I_f is the filtered insulin injection (insulin injection times the finite impulse response function), and similarly C_f is the filtered CHO intake. $\Phi[G(t)]$ is an autoregressive component consisting of a linear combination of *p* time-lagged values of blood glucose. Similarly, $\mathrm{B}[I_f(t)]$ and $\Gamma[C_f(t)]$ are autoregressive components consisting of *q* and *r* time lagged values of

filtered insulin and filtered CHO respectively. F is the finite impulse response function normalized to achieve the magnitude $||F||$ equal to one.

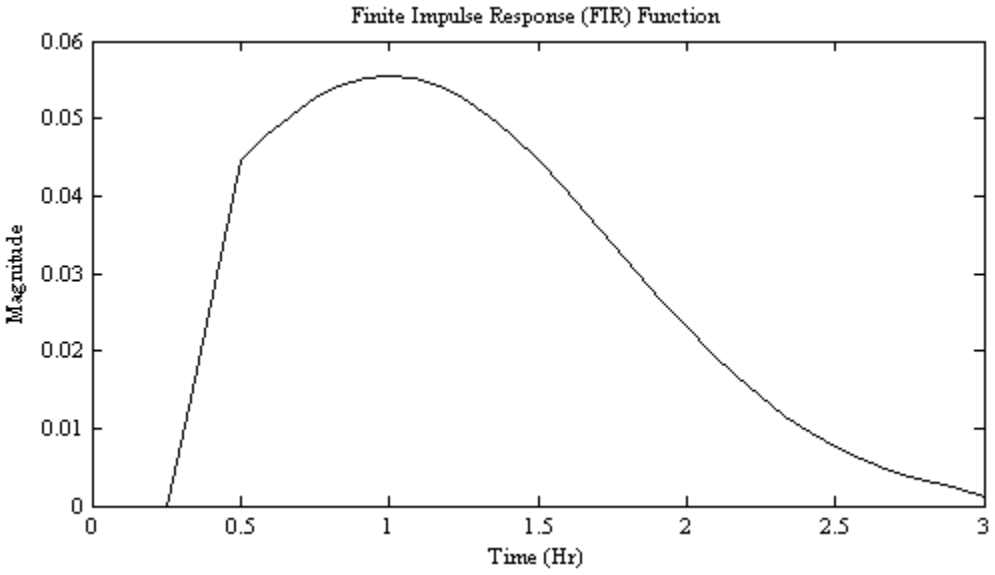

Figure 3.1: Normalized finite impulse response (FIR) function *F* from Equation 3-6 and Equation 3-7. Function adapted from [65, 95], normalization was added.

The FIR function (Equation 3-6 and Equation 3-7) is an averaged truncated Gaussian distribution. The mean and standard deviation were twelve and nine respectively. The dead time was five steps (25 minutes). After averaging and normalization, the resulting FIR function has a dead time *d* of three steps (15 min), a linear increase from three to six steps (15 to 30 min) and length of 36 steps (3 hours). The parameters *p*, *q*, and *r* were defined as two, six, and six respectively in [65, 95]. These selections will be maintained within this work and give the model 14 unknown parameters. The model memory states the amount of past information used in the calculation of the next step. For this model, it is defined as length of the FIR filter (36), plus the maximum of the parameters *q* and *r*,

minus one. For q and r equal to six, the model memory is 41 steps (205 minutes) This is very similar to the model memory of 36 steps (180 minutes) used in [68].

The model, although consisting of three components, does not have a compartmental structure. Unlike most other models, it is not built on first-order mass transfer equations between compartments. It is designed around the fact that insulin injection reduces blood glucose, carbohydrate (CHO) intake increases blood glucose and that both inputs have a time-lagged affect similar to the FIR filter. The exact magnitude and shape of their respective contributions to blood glucose are estimated through the state estimation routine. These assumptions are the only *a priori* assumptions made. The initial conditions of magnitude and covariance, for the unknown parameters, are the only *a posteriori* assumptions made. This data-driven modeling is especially beneficial in this case due to the high order and time varying nature of the glucose regulatory system (GRS).

In [65, 95], a second-order extended kalman filter [6] was used for parameter estimation. In this thesis, a standard first order kalman filter is used [34]. This will be shown to be an adequate estimator for parameter identification, while simultaneously reducing complexity. Persistency of excitation may be the biggest problem for estimation of this system. The CSII plus bolus approach to glucose control was used in the clinical data. This method, due to the relatively constant basal injection may satisfy persistency requirements, while algorithm determined control may not. There are major consequences of forcing persistent excitation of the GRS during closed loop control.

Without persistent excitation, parameters cannot be accurately identified, potentially resulting in poor forward prediction and thus control. With persistent excitation, hypoglycemia may result due to over medication. Conditions for defining persistence excitation can be found in [5].

3.3 Adaptive Dual Control

Dual control is an adaptive estimation and control technique in which (1) "the system output *cautiously* tracks the desired reference value" and (2) "it *excites* the plant sufficiently for accelerating the parameter estimation process" as to improve future controller performance [34]. These two main functions give the technique its name.

Traditionally, adaptive estimation and control were done in an uncoupled manner, where the controller is not designed to minimize the estimation error. This method has been referred to as the certainty-equivalence approach and has historically been the most widely used adaptive estimation and control method in applications. This method may be unfavorable for diabetes control due do the "turn-off" effect which occurs when the states of the system reach an equilibrium point and parameter estimation, and thus adaptation, slows. This "turn-off" effect also refers to the determinant of the information matrix approaching zero; which has been known to cause unrealistically large and fast adaptations [34].

In determining control action for insulin delivery in this work, we follow a bicriterial synthesis method and design a dual version of the Self-Tuning Regulator (section 4.2 in

[34]). The method involves minimizing two separate cost functions. The control losses are first minimized, given by Equation 3-10, which results in the cautious control action $u_c(k)$. The second cost function, Equation 3-11, is minimized in a domain around the cautious control, resulting in the dual control which is to be implemented on the system.

$$J_k^c = E\left\{\begin{matrix}\left[w(k+1)-y(k+1)\right]^2+\ldots \\ \ldots r\left[u(k)+q_1u(k-1)+\ldots+q_{n_Q}u(k-n_Q)\right]^2\end{matrix}\right\} \quad \textbf{Equation 3-10}$$

$$J_k^a = -E\left\{\left[y(k+1)-\hat{p}^T(k)m(k)\right]^2\right\} \quad \textbf{Equation 3-11}$$

where E denotes the expectation, w is the set-point or target value, y is the system output, r & q_i are weighting parameters, u is the system input, $\hat{p}$ is a vector of system parameter estimates, m is a vector of inputs and measured outputs and $\hat{p}^T m$ is the output prediction.

3.4 Connecting the Model and Dual Controller

For experimental evaluation, the estimation and control of the adaptive dual control should be applied to the real patient, possibly in a clinical setting. That is, the insulin delivery, carbohydrate (CHO) intake of the patient together with the glucose measurement of the patient will be used for estimation of the patient model; and then, based on the estimated patient model, the insulin determined by the adaptive control will be delivered to the real patient. However, in this work, clinical evaluation of the dual controller was not conducted, i.e. the application of the dual-control generated insulin to the real patient, and glucose level measurement from the real patient resulted from the control-generated insulin delivery were not implemented. Instead, simulations are used to evaluate the dual controller. In the simulations conducted in this thesis, a virtual patient is

generated, which is the data-driven linear, time-varying GRS model given in Equation 3-1 to Equation 3-9, derived using a first-order Kalman filter using clinically obtained data. This virtual patient model is similar to the work presented in [65], by our research group, except a lower-order estimation routine was used in this thesis. This virtual patient simply defined a multi-input/single output (MISO) relationship which could accurately simulate the dynamics of the glucose regulatory system (GRS). Carbohydrate (CHO) intake is the disturbance input and insulin injection is the control input, and blood glucose is the single output. The virtual patient is fully defined by the coefficients φ_i, β_i, and γ_i in the model described in section 3.2 and as described in [65]. The quality of fit for the virtual patient is presented in section 4.1 of this thesis. In the future, evaluation of the adaptive controller using a FDA-approved simulation platform is planned.

As shown in Figure 3.2, at each iteration of the adaptive dual control, the model parameters, $\hat{p}$ (in Equation 3-12), are estimated and then used in the implementation of the dual controller. This estimation derives the model coefficients from the data provided to, and returned from, the virtual patient. Then the estimated parameters are used to derive the cautious control by minimizing the cost function Equation 3-10. An additional control is derived to minimize the estimation error (cost function in Equation 3-11). The dual control is obtained by the cautious control and the additional control which is then fed to the virtual patient. The process then repeats. Initial conditions of blood glucose, CHO intake and insulin delivery were taken from the clinical data in both cases (virtual patient and adaptive control). A flow chart displaying the main operations in the process is shown in Figure 3.2 below

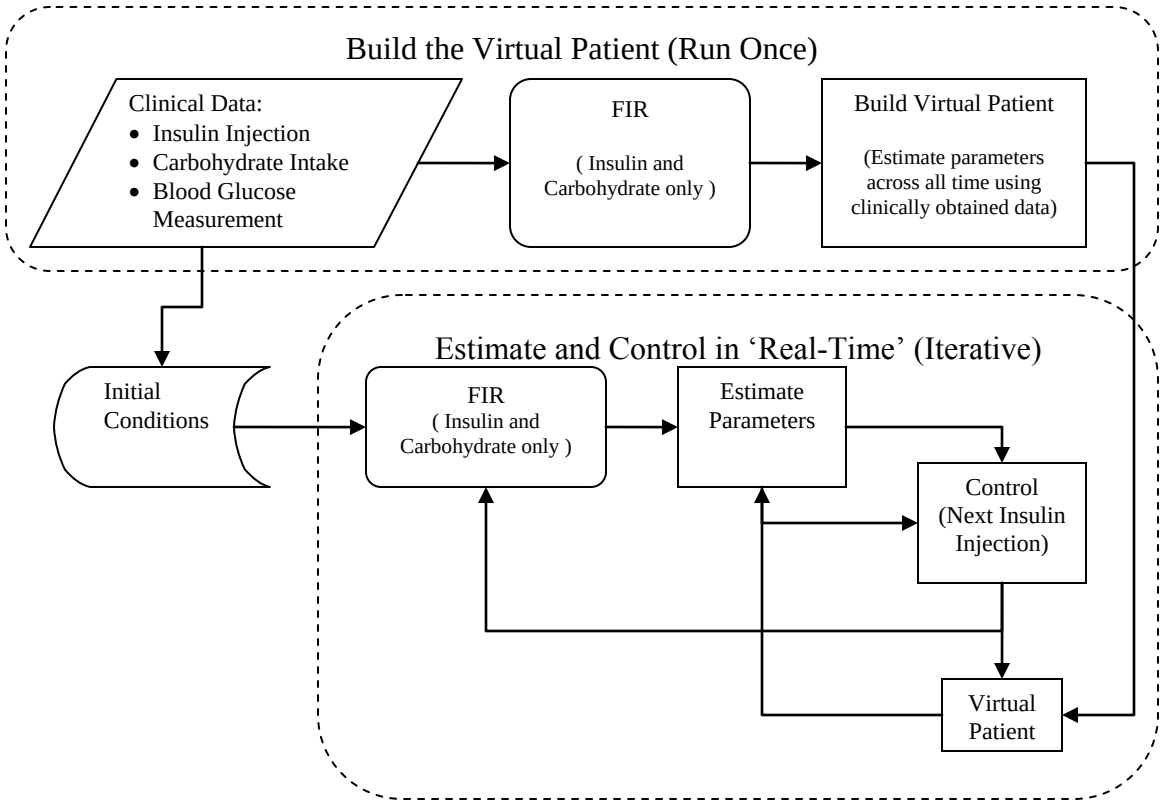

Figure 3.2: Flow chart of the modeling and control process. The virtual patient serves as the I/O model of the glucose regulatory system (GRS) replacing a real patient.

3.5 Design of Adaptive Dual Control for the Linear Time-Varying GRS Model

In terms of Equation 3-1 through Equation 3-9, define

$$p_e(k) = \left[\phi(1:p) \quad \beta(1:q) \quad \gamma(1:r)\right] \qquad \textbf{Equation 3-12}$$

$$m_e(k) = \left[BG(k), BG(k-1), I_f(k) \ldots I_f(k-5), C_f(k) \ldots C_f(k-5)\right] \qquad \textbf{Equation 3-13}$$

Then we have

$$y(k+1) = BG(k+1) = p_e(k)^T m_e(k) + \varepsilon(k) \qquad \textbf{Equation 3-14}$$

where $\varepsilon(k)$ denotes the measurement noise and the subscript e denotes the form used within the estimation routine. For parameter estimation, a standard first order kalman

filter (as opposed to a 2nd-order extended kalman filter, used in [65]) is used and is given by Equation 3-15 through Equation 3-18 assuming $p_e(k+1)=p_e(k)+\xi(k)$, where $\xi(k)$ denotes the process noise in the state equation for $p_e(k)$.

$$\hat{p}_e(k+1) = \hat{p}_e(k) + q(k+1)e(k+1) \quad \textbf{Equation 3-15}$$

$$e(k+1) = y(k+1) - \hat{p}_e^T(k)m_e(k) \quad \textbf{Equation 3-16}$$

$$q(k+1) = P_e(k)m_e(k)\left[m_e^T(k)P_e(k)m_e(k) + \sigma_\xi^2\right]^{-1} \quad \textbf{Equation 3-17}$$

$$P_e(k+1) = P_e(k) - q(k+1)m_e^T(k)P_e(k) + Q_\xi(k) \quad \textbf{Equation 3-18}$$

where, e denotes the estimation error, $\hat{p}_e$ is a vector of system parameter estimates of p_e, P_e is the corresponding covariance matrix for the state vector p_e, σ_ξ denotes the standard deviation of the process noise, and Q_ξ denotes the covariance matrix associated with the process noise. Generally, covariance matrices provide a measure of how much variables change with respect to each other. Specifically, the covariance between two real valued random variables X and Y is given by Equation 3-19 where $E[X]$ denotes the expected value of X.

$$Cov(X,Y) = E\left[\left(X - E\left[X\right]\right)\left(Y - E\left[Y\right]\right)\right] \quad \textbf{Equation 3-19}$$

Note that in Equation 3-13, the input variables in the I/O format used for estimation include both filtered insulin delivery rate and filtered carbohydrate intake, while the real control variable to the diabetic patient, which needs to be determined by the adaptive dual controller (considering the cost functions in Equation 3-10 and Equation 3-11) is the non-filtered insulin delivery rate. Consequently, we re-write the I/O model given by Equation 3-12 through Equation 3-14 into a new I/O format as follows (with subscript c to denote

that it is for control purpose). By taking into account the delay factor of the insulin delivery, we define

$$p_c(k) = \left[b_1(k-d) \vdots p_0^T(k) \right]^T \quad \textbf{Equation 3-20}$$

$$m_c(k) = \left[u(k-d) \vdots m_0^T(k) \right]^T \quad \textbf{Equation 3-21}$$

$$P_c(k) = \begin{bmatrix} p_{b1}(k) & p_{b1p0}^T(k) \\ p_{b1p0}(k) & P_{P0}(k) \end{bmatrix} \quad \textbf{Equation 3-22}$$

where *u(k-d)* corresponds to insulin delivery at the time instant *k-d* with time delay *d*, $b_1(k-d)$ is the coefficient associated with the control input at time *k-d*. The vectors p_c and m_c and their corresponding partitions should satisfy Equation 3-23.

$$BG(k+1) = p_c(k)^T m_c(k) + \varepsilon(k) \quad \textbf{Equation 3-23}$$

The covariance matrix P_c for p_c is defined accordingly in terms of the partition of p_c and m_c, with p_{b1} being a scalar corresponding to the covariance of b_1.

In the design of the adaptive dual controller for the virtual patient, we consider the cost functions defined in Equation 3-10 and Equation 3-11 for minimizing the tracking error (cautions control) and minimizing estimation errors. For the glucose control, the output *y(k+1)* is *BG(k+1)*, and *w(k+1)* denotes the target glucose level at *(k+1)* time instant; the control input *u(k)* denotes the insulin delivery at time instant *k*. It should be noted that for Equation 3-11, in terms of the two I/O representations (p_e, m_e, P_e) and (p_c, m_c, P_c), we have

$$\hat{y} = \hat{p}_c^T(k) m_c(k) = \hat{p}_e^T(k) m_e(k) \quad \textbf{Equation 3-24}$$

In order to derive the control variable *u(k)* in terms of the new I/O format (p_c, m_c, P_c) to minimize the cost functions, the covariance matrix $P_c(k)$ in terms of $p_c(k)$ has to be computed from $P_e(k)$ given in Equation 3-18. Fortunately, only the first row and diagonal elements of the new covariance matrix P_c need to be computed in the derivation of the adaptive dual control. The computation of m_c, p_c and P_c in terms of m_e, p_e, and P_e is given as follows,

$$m_c(k) = \left[I(k-d) : I(k-m), BG(k), BG(k-1), \Gamma\left[C_f(k)\right] \right]^T \qquad \textbf{Equation 3-25}$$

$$p_c(k) = \begin{bmatrix} \beta_1 F(4) \\ \beta_1 F(5) + \beta_2 F(4) \\ \beta_1 F(6) + \beta_2 F(5) + \beta_3 F(4) \\ \beta_1 F(7) + \beta_2 F(6) + \beta_3 F(5) + \beta_4 F(4) \\ \beta_1 F(8) + \beta_2 F(7) + \beta_3 F(6) + \beta_4 F(5) + \beta_5 F(4) \\ \beta_1 F(9) + \beta_2 F(8) + \beta_3 F(7) + \beta_4 F(6) + \beta_5 F(5) + \beta_6 F(4) \\ \beta_1 F(10) + \beta_2 F(9) + \beta_3 F(8) + \beta_4 F(7) + \beta_5 F(6) + \beta_6 F(5) \\ \vdots \\ \beta_1 F(36) + \beta_2 F(35) + \beta_3 F(34) + \beta_4 F(33) + \beta_5 F(32) + \beta_6 F(31) \\ \beta_2 F(36) + \beta_3 F(35) + \beta_4 F(34) + \beta_5 F(33) + \beta_6 F(32) \\ \beta_3 F(36) + \beta_4 F(35) + \beta_5 F(34) + \beta_6 F(33) \\ \beta_4 F(36) + \beta_5 F(35) + \beta_6 F(34) \\ \beta_5 F(36) + \beta_6 F(35) \\ \beta_6 F(36) \\ \phi_1 \\ \phi_2 \\ 1 \end{bmatrix} \qquad \textbf{Equation 3-26}$$

$$P_c(1,:,k) = \begin{bmatrix} P_e(3,3,k)F(4)^2 \\ \left[P_e(3,3:4,k)\right]\left[F(5:-1:4)\right]^T F(4) \\ \left[P_e(3,3:5,k)\right]\left[F(6:-1:4)\right]^T F(4) \\ \left[P_e(3,3:6,k)\right]\left[F(7:-1:4)\right]^T F(4) \\ \left[P_e(3,3:7,k)\right]\left[F(8:-1:4)\right]^T F(4) \\ \left[P_e(3,3:8,k)\right]\left[F(9:-1:4)\right]^T F(4) \\ \left[P_e(3,3:8,k)\right]\left[F(10:-1:5)\right]^T F(4) \\ \vdots \\ \left[P_e(3,3:8,k)\right]\left[F(36:-1:31)\right]^T F(4) \\ \left[P_e(3,4:8,k)\right]\left[F(36:-1:32)\right]^T F(4) \\ \left[P_e(3,5:8,k)\right]\left[F(36:-1:33)\right]^T F(4) \\ \left[P_e(3,6:8,k)\right]\left[F(36:-1:34)\right]^T F(4) \\ \left[P_e(3,7:8,k)\right]\left[F(36:-1:35)\right]^T F(4) \\ P_e(3,8,k)F(36)F(4) \\ P_e(3,1,k)F(4) \\ P_e(3,2,k)F(4) \\ sum\left(P_e(3,9:14,k)\right)F(4) \end{bmatrix}^T \quad \textbf{Equation 3-27}$$

$$
diag\left(P_c(:,:,k)\right) = \begin{bmatrix}
P_e(3,3,k)F(4)^2 \\
\left[P_e(3,3:4,k)\right]\left[F(5:-1:4)^2\right]^T + 2P_e(3,4,k)F(4)F(5) \\
\left[P_e(3,3:5,k)\right]\left[F(6:-1:4)^2\right]^T + \dots \\
\dots 2\begin{pmatrix} P_e(3,4,k)F(6)F(5) + P_e(3,5,k)F(6)F(4)\dots \\ + P_e(4,5,k)F(5)F(4) \end{pmatrix} \\
\left[P_e(3,3:6,k)\right]\left[F(7:-1:4)^2\right]^T + \dots \\
\dots 2\begin{pmatrix} P_e(3,4,k)F(7)F(6) + P_e(3,5,k)F(7)F(5)\dots \\ + P_e(3,6,k)F(7)F(4) + P_e(4,5,k)F(6)F(5)\dots \\ + P_e(4,6,k)F(6)F(4) + P_e(5,6,k)F(5)F(4) \end{pmatrix} \\
\vdots \\
\left[P_e(3,5:8,k)\right]\left[F(36:-1:33)^2\right]^T + \dots \\
\dots 2\begin{pmatrix} P_e(5,6,k)F(36)F(35) + P_e(5,7,k)F(36)F(34)\dots \\ + P_e(5,8,k)F(36)F(33) + P_e(6,7,k)F(35)F(34)\dots \\ + P_e(6,8,k)F(35)F(33) + P_e(7,8,k)F(34)F(33) \end{pmatrix} \\
\left[P_e(3,6:8,k)\right]\left[F(36:-1:34)^2\right]^T + \dots \\
\dots 2\begin{pmatrix} P_e(6,7,k)F(36)F(35) + P_e(6,8,k)F(36)F(34)\dots \\ + P_e(7,8,k)F(35)F(34) \end{pmatrix} \\
\left[P_e(3,7:8,k)\right]\left[F(36:-1:35)^2\right]^T + 2P_e(7,8,k)F(36)F(35) \\
P_e(8,8,k)F(36)^2 \\
P_e(1,1,k) \\
P_e(2,2,k) \\
sum\left(diag\left(P_e(9:14,9:14,k)\right)\right)
\end{bmatrix}^T
$$

Equation 3-28

where $\Gamma[C_f(k)]$ is the accumulated carbohydrate contribution towards blood glucose (calculated by Equation 3-5), parameters φ_i and β_i in Equation 3-26 are $\varphi_i(k)$ and $\beta_i(k)$ respectively (the time index was omitted to make the notation concise), P_e is the covariance matrix resulting from parameter estimation, $P_c(1,:,k)$ is the first row of the transformed covariance matrix P_c and $diag(P_c(:,:,k))$ is a vector of the diagonal elements of the transformed covariance matrix P_c.

The design of the dual control is described as follows. First the cautious control is calculated by substituting Equation 3-14 into Equation 3-10 and then taking the expectation. After setting the derivative with respect to the control input, $u(k\text{-}d)$, equal to zero, the cautious control, denoted by $\underline{u_c}$, takes the form shown in Equation 3-29. After the cautious control is obtained, the second cost function (Equation 3-11) is minimized in the region around the cautious control.

$$u_c(k) = \frac{\begin{bmatrix} \hat{b}_1(k-d)w(k+1)... \\ ... - \left[\hat{b}_1(k-d)\,p_0^T(k) + p_{b_1 p_0}(k)\right] m_0(k) + r\bar{u}(k-d-1) \end{bmatrix}}{\hat{b}_1^2(k-d) + p_{b_1}(k) + r} \qquad \textbf{Equation 3-29}$$

$$\bar{u}(k-d-1) = q_1 u(k-d-1) + \ldots + q_{n_Q} u(k-d-n_Q) \qquad \textbf{Equation 3-30}$$

$$u(k) = u_c(k) + \theta(k)\,sign\left[p_{b_1}(k)u_c(k) + p_{b_1 p_0}^T(k)m_0(k)\right] \qquad \textbf{Equation 3-31}$$

$$\theta(k) = \eta \cdot trace\{P_c(k)\}, \eta \geq 0 \qquad \textbf{Equation 3-32}$$

$$\Omega(k) = \left[u_c(k) - \theta(k); u_c(k) + \theta(k)\right] \qquad \textbf{Equation 3-33}$$

where u_c is the cautious control, u is the final dual control, w is the target or set-point value (constant in this design), Ω is the range for the dual control around the cautious control, d is the delay time, and $q_i\,(i=1{:}n_Q)$, r & η are design parameters.

Two hard constraints are imposed on the control input. First, the control input (insulin injection) must be greater than or equal to zero. This is a physical constraint because once insulin is delivered, it cannot be retrieved. The second constraint is added as a safety measure to reduce the occurrence of hypoglycemia. It states that if the blood glucose concentration is below the target value, then no insulin should need to be injected. These two constraints might limit the input signal from the dual control

algorithm which tries to maintain persistent excitation and thus could reduce the efficiency of accurate estimation.

According to Filatov and Unbehauen [34], “the strict convergence and stability analysis of the considered adaptive systems {adaptive dual control} presents a difficult problem that cannot be solved analytically for the general case presently”. Additionally, they noted the importance of checking for convergence via computer simulations. The simulations requested for assessing stability and convergence of adaptive systems are performed within thesis. Further discussion is presented in the next chapter.

Chapter 4: Simulation Results

This chapter focuses on performance evaluation of modeling the GRS, parameter estimation and the adaptive dual controller. First the virtual patient model is given and the quality of the model is evaluated in terms of and goodness-of-fit of the parameter estimation, for which a correlation coefficient *R*, is computed between the clinically measured data and a 6-step (30 minute) forward prediction of the blood glucose concentration. Generally, correlation coefficients have values ranging from -1 to 1 and signify how related two variables are; with 1 being perfectly related, -1 being inversely related and 0 being no relation. The correlation coefficient *R* is given by Equation 4-1, where *X*, in this case, is the measured blood glucose and *Y* is the 6-step (30 minute) forward prediction of the blood glucose concentration; $\overline{X}$ and $\overline{Y}$ are the mean values of *X* and *Y* respectively, *n* is the number of measurements.

$$R = \frac{\sum_{i=1}^{n}\left[(X_i - \overline{X})(Y_i - \overline{Y})\right]}{\sqrt{\sum_{i=1}^{n}(X_i - \overline{X})^2}\sqrt{\sum_{i=1}^{n}(Y_i - \overline{Y})^2}} \qquad \textbf{Equation 4-1}$$

The performance evaluation of the interconnected parameter estimation and adaptive dual controller will be given in terms of the statistics and metrics outlined in section 2.4 of this thesis.

4.1 Virtual Patients

As in [65], virtual patients were created from all five data-sets. Correlation coefficients using the first-order kalman filter were not significantly different to that achieved in [65], in which a second order extended kalman filter was used (see Table 4.1) in terms of

two-tailed Student t-tests with the significance level α set to 0.1, defined by Equation 4-2 where c is the confidence level between zero and one). Throughout this thesis, the measurement error was assumed to be a normally distributed random variable with a mean of zero and standard deviation of two mg/dl. This value is rather arbitrary. The literature suggests a large, partially biased, measurement error for the CGMS device (mean absolute deviation was 15-20%) [41], while the clinically measured data seems to have minimal random error (determined by eye, references values were not recorded).

$$\alpha = (1 - c) \qquad \textbf{Equation 4-2}$$

Virtual Patient No.	6-Step Ahead Correlation Coefficient "R" [65]	6-Step Ahead Correlation Coefficient "R" [This thesis]
1	0.84	0.82
2	0.97	0.95
3	0.93	0.86
4	0.92	0.88
5	0.91	0.88
Mean	0.91	0.88
St.D.	0.05	0.05

Table 4.1: Correlation coefficients between six-step step (30-min) ahead forward model predictions and measured blood glucose values

In Figure 4.5 through Figure 4.5, the clinical data for all five patients is plotted against virtual patient model predictions. Note that the blood glucose prediction is for 6-steps or 30 minutes in the future for each time step. The clinically determined insulin injection and carbohydrate (CHO) intake is shown in black in subplots 2 and 3 of the above

mentioned figures. Their time-delayed effects towards the blood glucose prediction is shown in red and plotted on a separate ordinate axis. Also note that insulin injection always has a negative contribution to the blood glucose and that (CHO) always has a positive contribution to blood glucose. Due to some lapses in the three days of clinically acquired data, the longest uninterrupted time period of data was used for each patient making the length of prediction different for each patient. The length of each uninterrupted data set was 49.00, 64.92, 49.08, 62.33, and 70.83 hours for patient's one through five respectively.

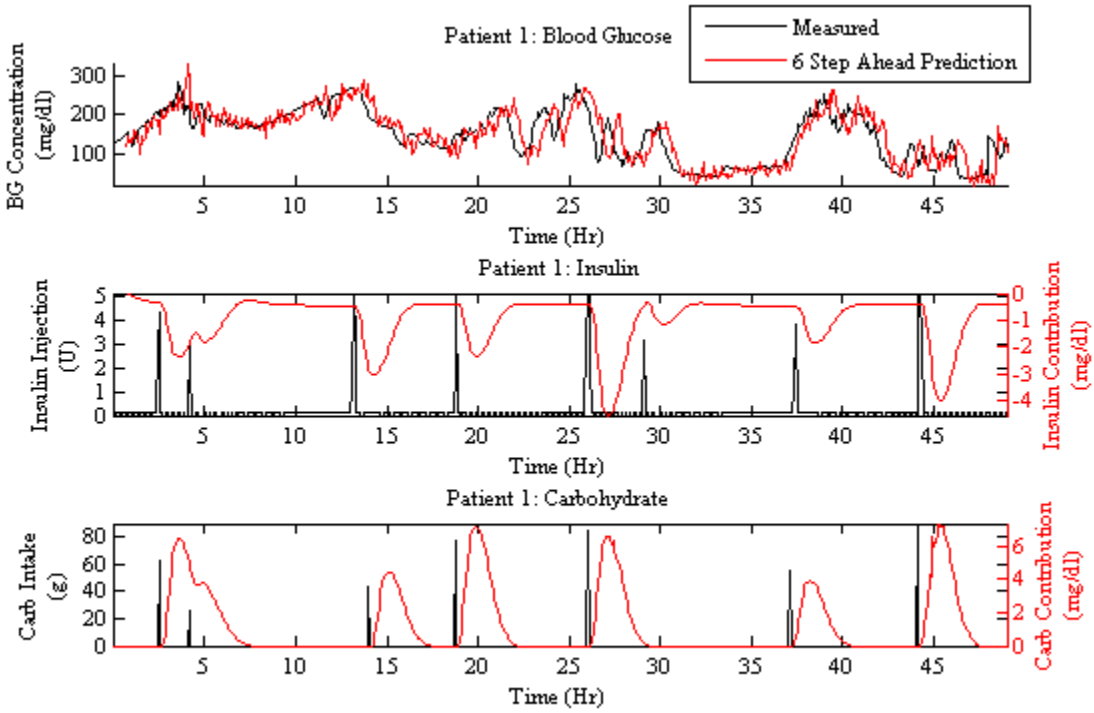

Figure 4.1: Virtual Patient 1, blood glucose prediction is for 6-steps (30 min.) forward in time, Insulin and CHO Contributions are time delayed responses, blood glucose measurement error is assumed to be normally distributed with zero mean and standard deviation of 2 mg/dl

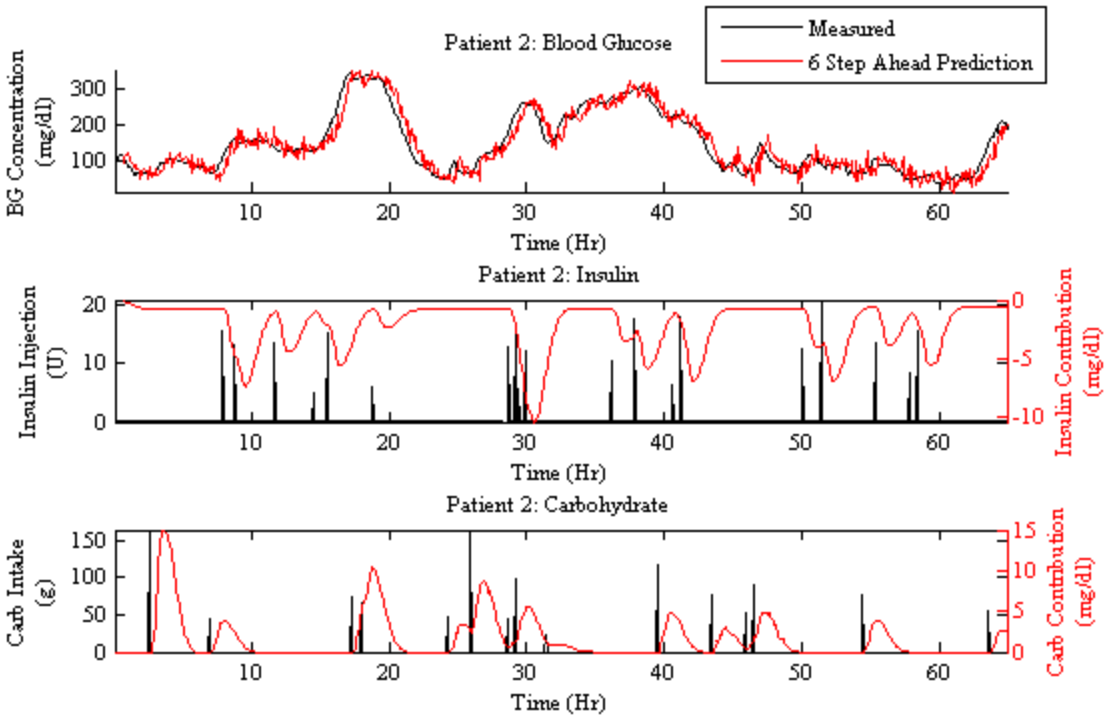

Figure 4.2: Virtual Patient 2

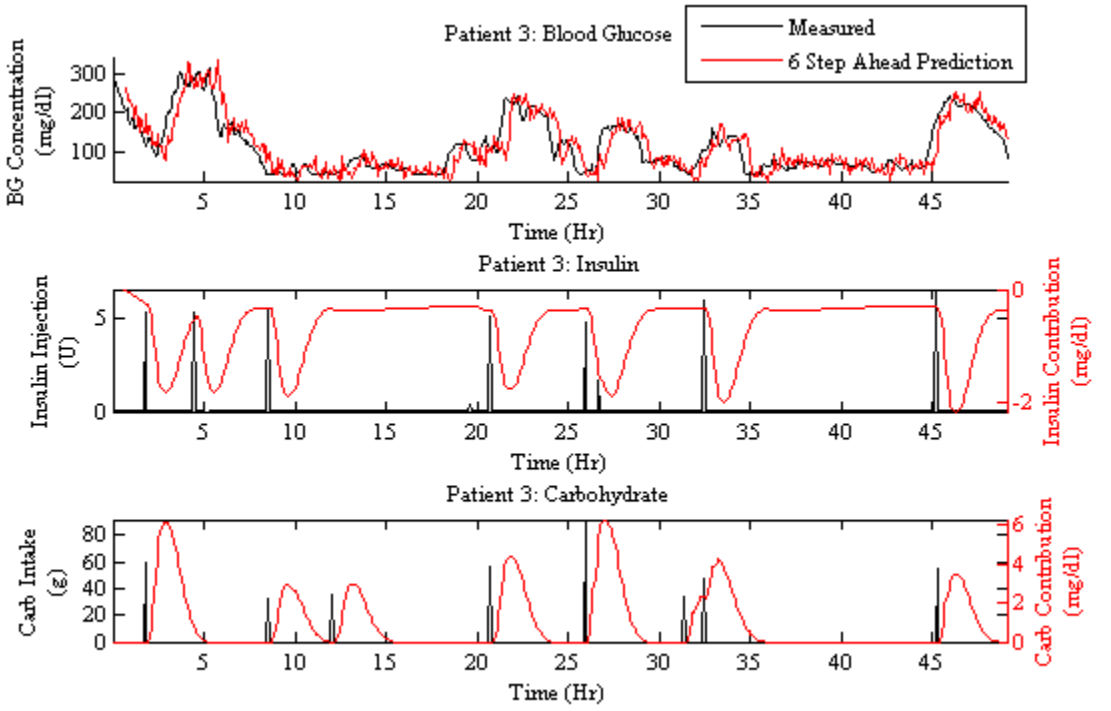

Figure 4.3: Virtual Patient 3

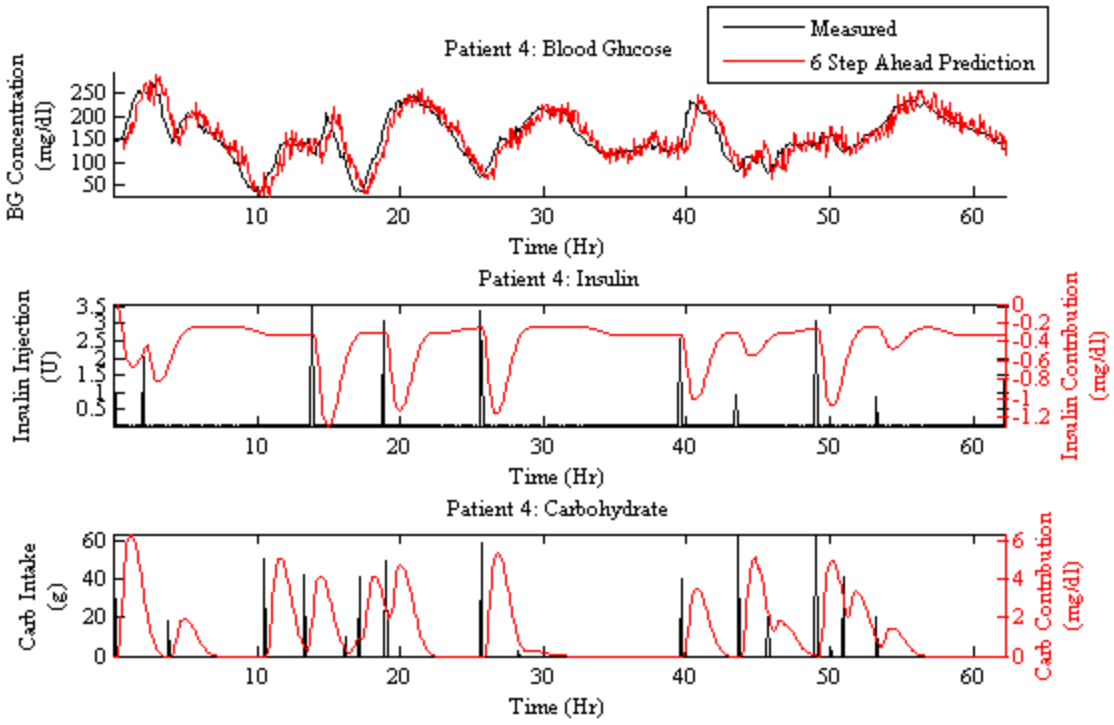

Figure 4.4: Virtual Patient 4

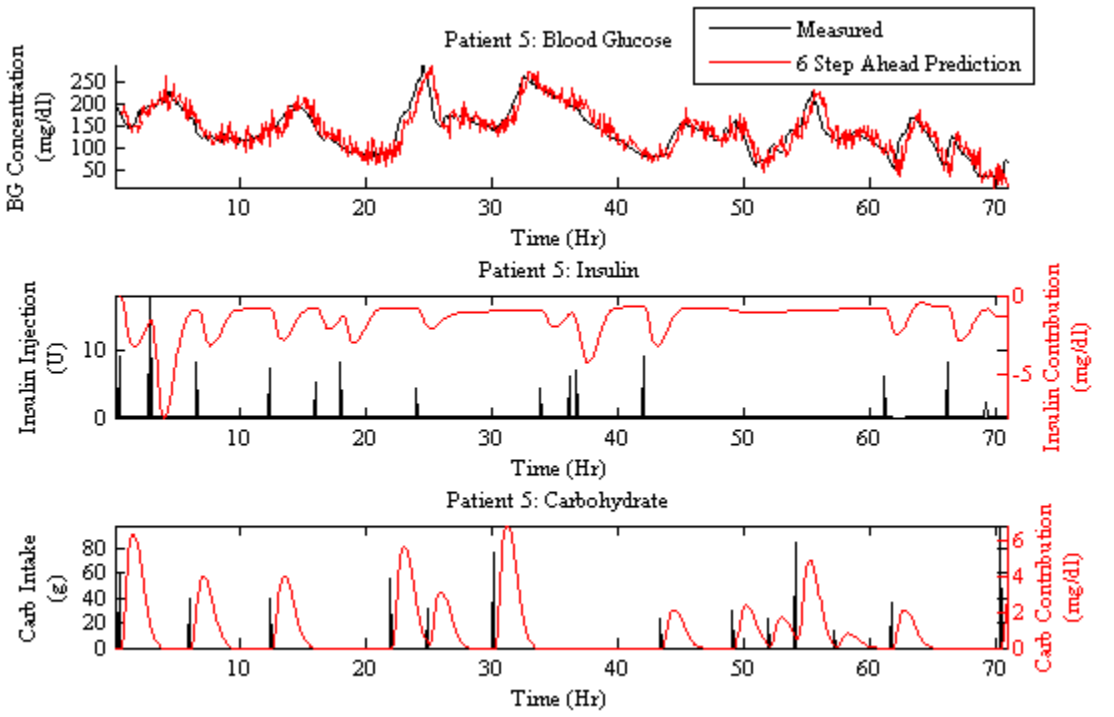

Figure 4.5: Virtual patient 5

The parameter estimates for all five patients are given in Figure 4.6 through Figure 4.10. The initial values of the unknown parameters used in the estimation are given in Table 4.2 (used for all patient datasets). The initial values of the covariance matrix were chosen randomly from a normally distributed function with zero mean and standard deviation of 0.01 (the same set of random covariance initial conditions were used for all patient datasets by setting the random number stream to the default value in MATLAB). Note below the time-varying behavior of the estimated parameters.

Unknown Parameter	Initial Value
φ_1	0.8
φ_2	0.2
β_i (i=1,…,6)	-5/6
γ_i (i=1,…,6)	2/6

Table 4.2: Initial parameter values. Note: all β's and all γ's have the same initial value

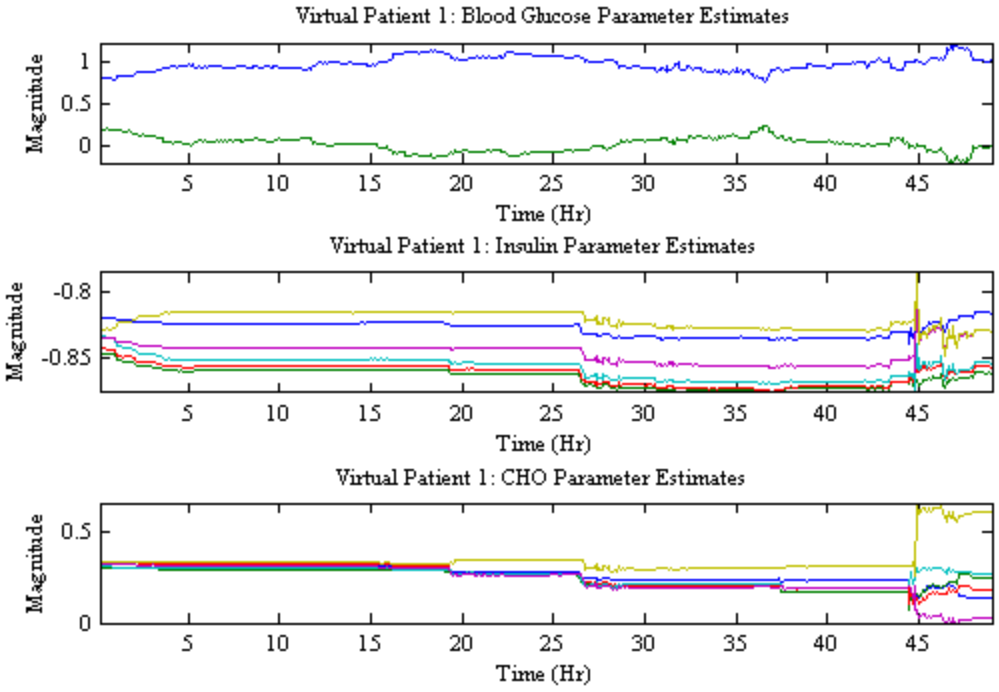

Figure 4.6: Parameter estimates for virtual patient 1 using clinical data. For the sake of space, legends have been omitted. Subplot 1 contains the φ parameters, subplot 2 contains the β parameters subplot 3 contains the γ parameters. The color of the parameters 1-6 is given by standard MATLAB color code (blue, green, red, cyan, magenta, yellow) respectively.

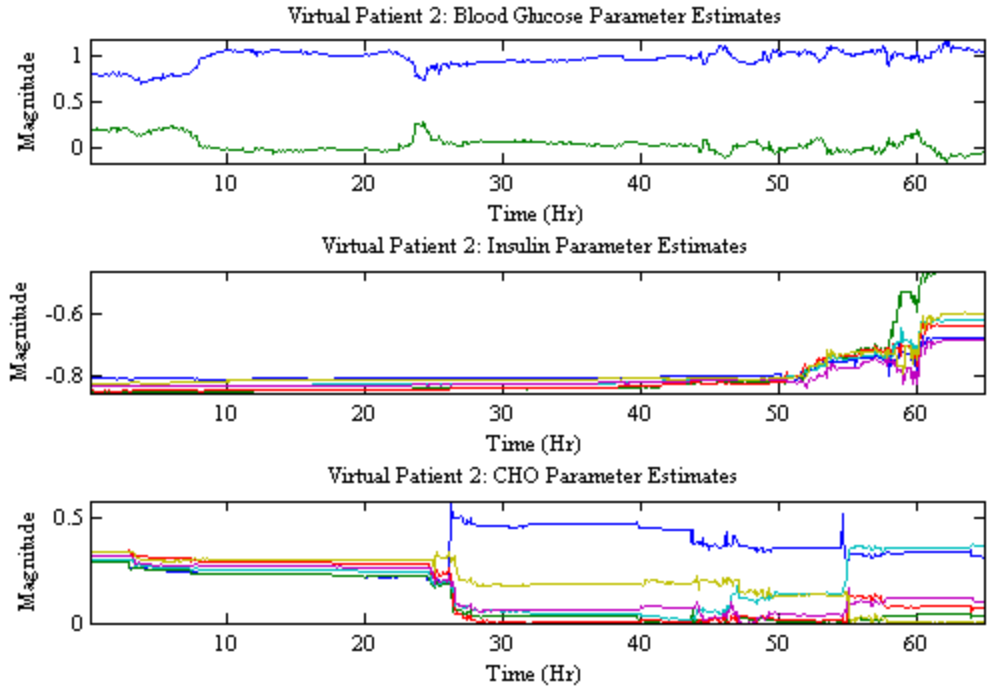

Figure 4.7: Parameter Estimates for Virtual Patient 2 using clinical data.

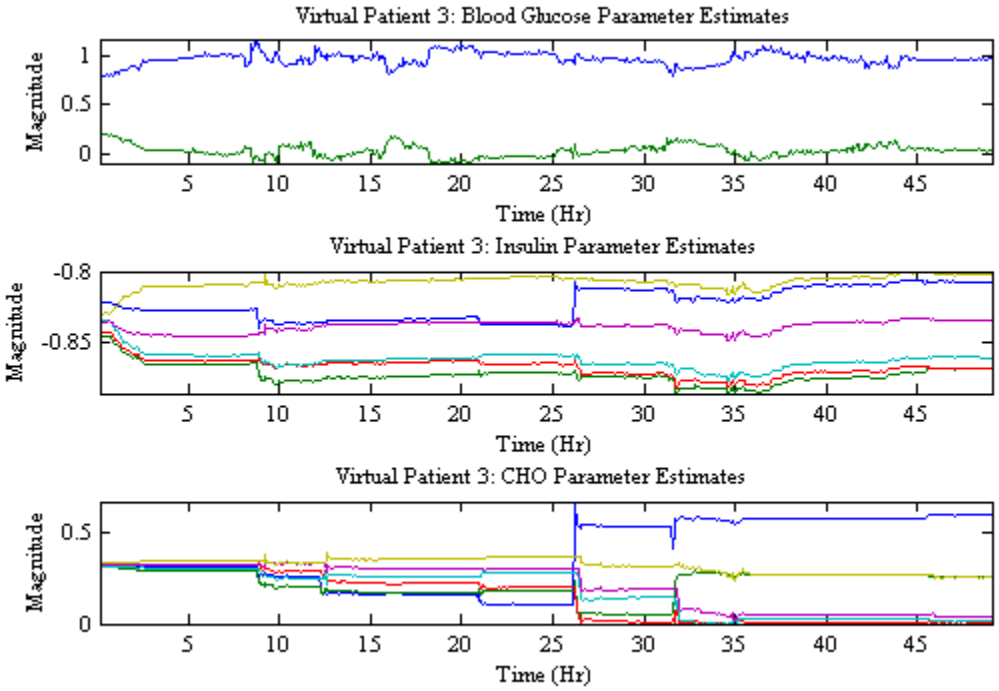

Figure 4.8: Parameter Estimates for Virtual Patient 3 using clinical data.

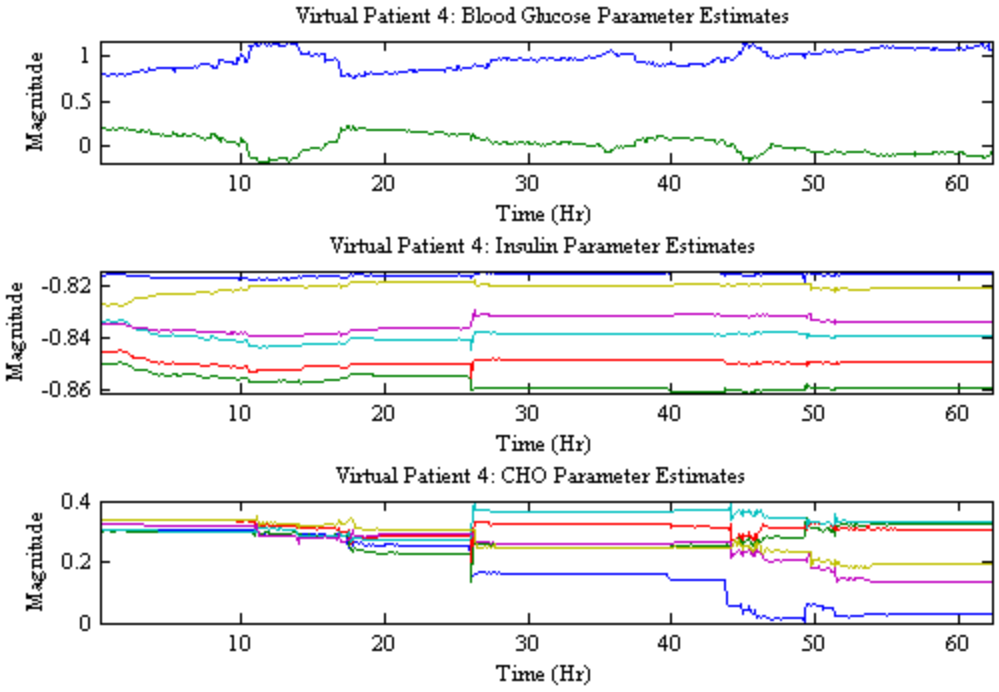

Figure 4.9: Parameter Estimates for Virtual Patient 4 using clinical data.

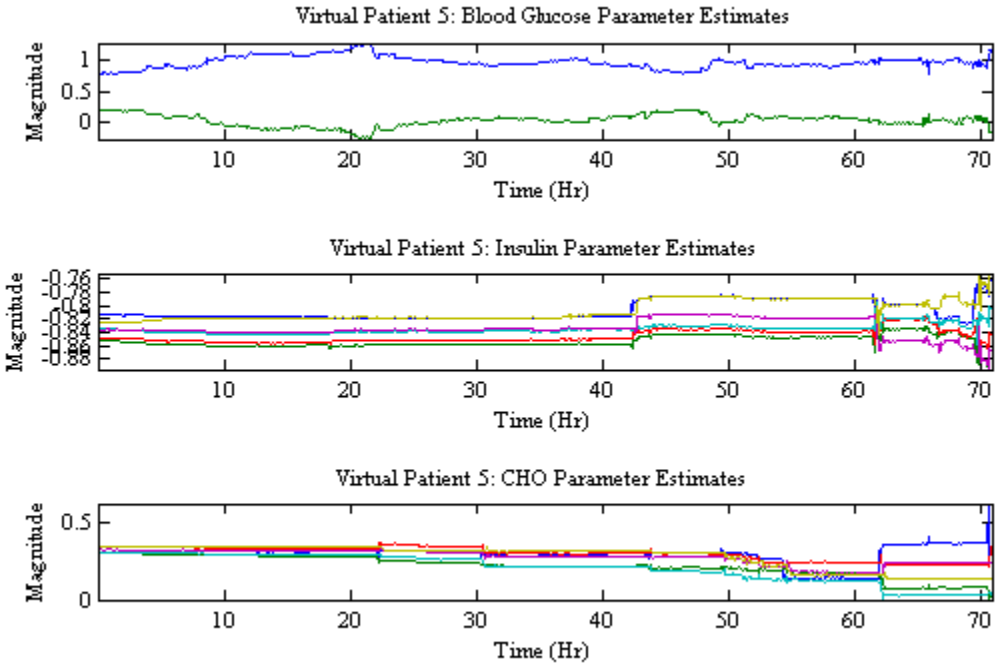

Figure 4.10: Parameter Estimates for Virtual Patient 5 using clinical data.

4.2 Adaptive Dual Control

The design parameters of the adaptive dual control were chosen on a trial and error basis. The following parameters were used for all patients in producing all the simulation results given in the section. In Equation 3-29 through Equation 3-32, $BG_{target} = w = 100$ mg/dl for all k, $r = 0.35$, $\eta = 0.1$, $n_Q = d+1 = 4$, $q_0 - q_{nQ} = 0.01$. Among the five patients: patients 1, 3, 4, and 5 show better performance than the clinical data (detailed information given below), while the control for patient 2 is not stable. The cause of the instability is not currently clear for this current stage of research; and the simulation results corresponding to patient two are thus omitted in the remainder of this thesis.

Figure 4.11 through Figure 4.14 show the simulated performance of the adaptive dual controller in terms of blood glucose (subplot 1), insulin delivery (subplot 2) and carbohydrate intake (subplot 3, taken from clinical data) for patients 1, 3, 4, and 5 respectively. Note that the black dotted lines in the second subplot of the above mentioned figures indicate the range of potential control around the cautious control. This range is given by Equation 3-33. The red dash-dotted lines in the second and third subplots (plotted on a second y-axis) indicate the 'actual' contributions of insulin and carbohydrate (CHO) towards blood glucose (see Equation 3-4 and Equation 3-5). These 'actual' contributions were determined by applying the insulin delivery determined by the dual control algorithm and CHO intake observed clinically to the virtual patient model; i.e. they are computed by the product of virtual patient insulin sensitivity parameters (β_i, i=1:6) and controlled insulin delivery, and the product of virtual patient carbohydrate sensitivity parameters ($\gamma_{i,}$ i=1:6) and the clinically observed CHO intake. The dashed red

lines indicate the contribution of the same insulin and CHO inputs as seen by adaptive dual control; i.e. they are calculated using online parameter estimates for the insulin and CHO sensitivities as opposed to those estimated offline for the virtual patient. The difference between the red dash-dotted lines and red dashed lines, in these subplots, is the realized difference in parameter estimation (between the virtual patient and online controller). In Figure 4.11 through Figure 4.14 there is almost no difference between the 'actual' insulin contribution (computed from the virtual patient) and the insulin contribution calculated with estimated parameters used in the online dual control algorithm. In these same figures, the difference in the carbohydrate contribution was significant; consistently resulting in, from the perspective of the controller, an underestimated carbohydrate affect towards blood glucose. This substantial underestimation makes closed loop control more difficult because it forecasts a smaller glucose excursion than which occurs within the virtual patient and thus what actually gets applied to the model. Considering this, the performance of the dual control algorithm appears very impressive.

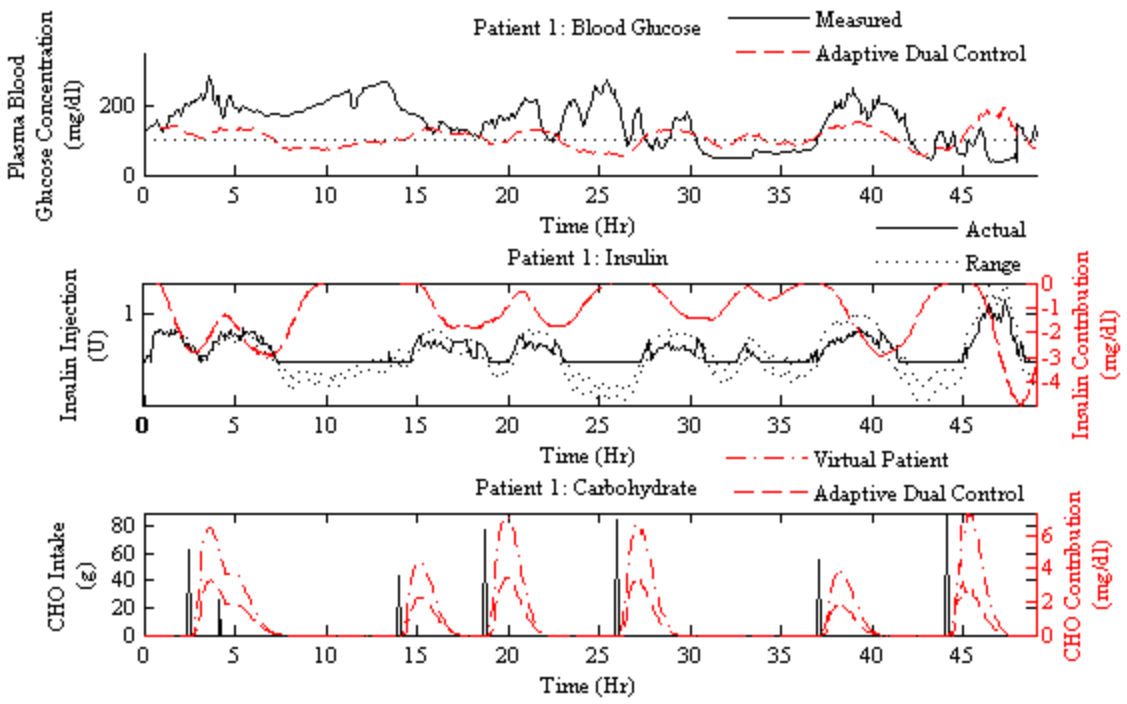

Figure 4.11: Simulated performance of adaptive dual control for patient 1. In subplot 1, the black solid line represents the clinically measured blood glucose concentration; the red dashed line represents the blood glucose concentration as outputted by the virtual patient model under the adaptive dual control. In subplot 2, the black solid line represents the final insulin delivery determined by the dual control algorithm, the black dotted lines are the range of possible dual control around the cautious control, the red dash-dotted line represents the corresponding insulin contribution computed from the virtual patient, and the red dashed line (almost perfectly overlapping the red dash-dotted line) is the cooresponding insulin contribution computed from the estimated parameters resulting from the online dual controller. In subplot 3, the black solid line represents the clinically observed carbohydrate intake, the red dash-dotted line represents the corresponding CHO contribution from the virtual patient, and the red dashed line represents the CHO contribution computed from parameter estimates from the online dual controller.

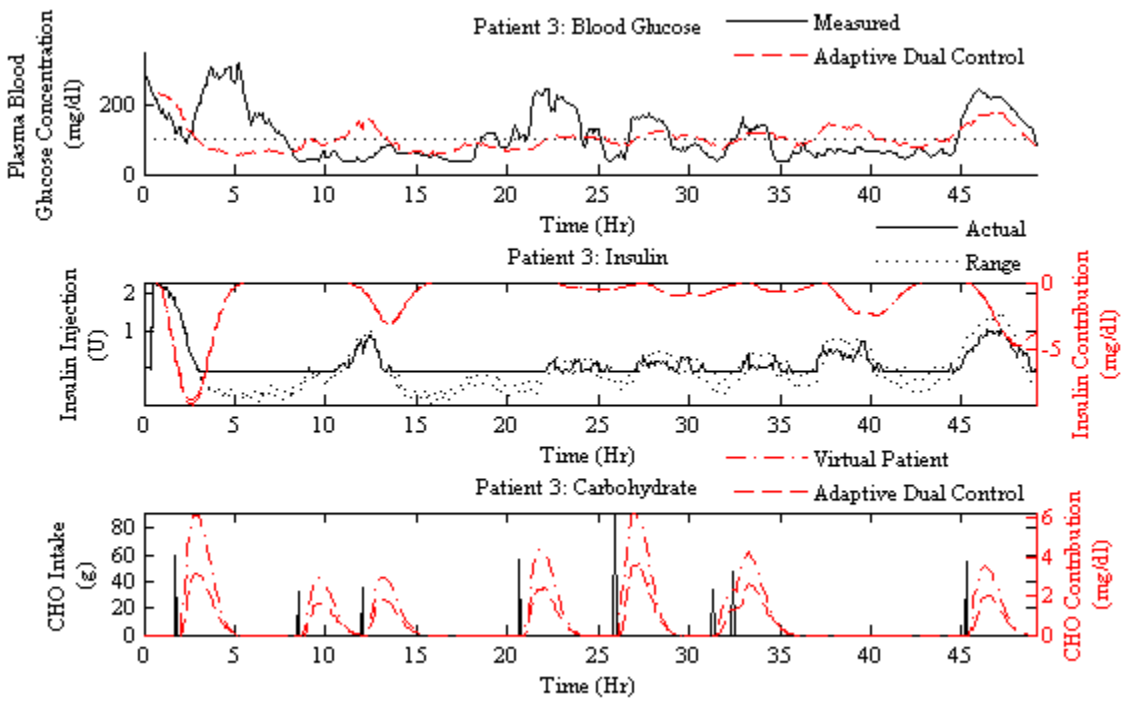

Figure 4.12: Simulated performance of adaptive dual control for patient 3.

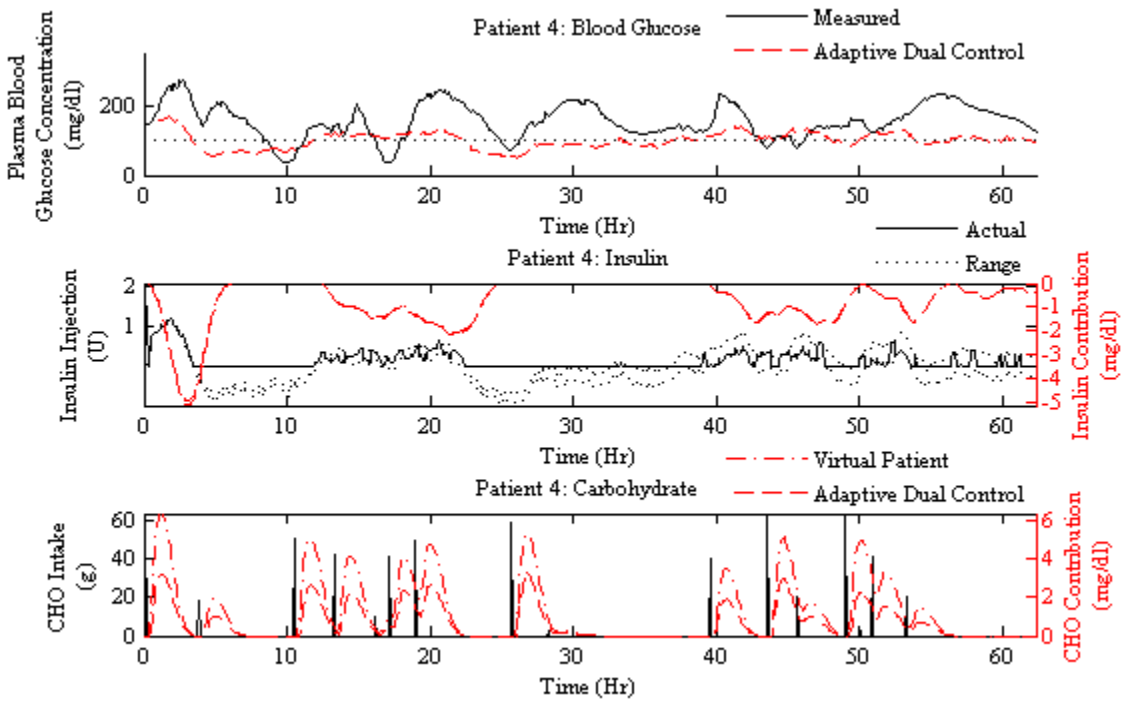

Figure 4.13: Simulated performance of adaptive dual control for patient 4.

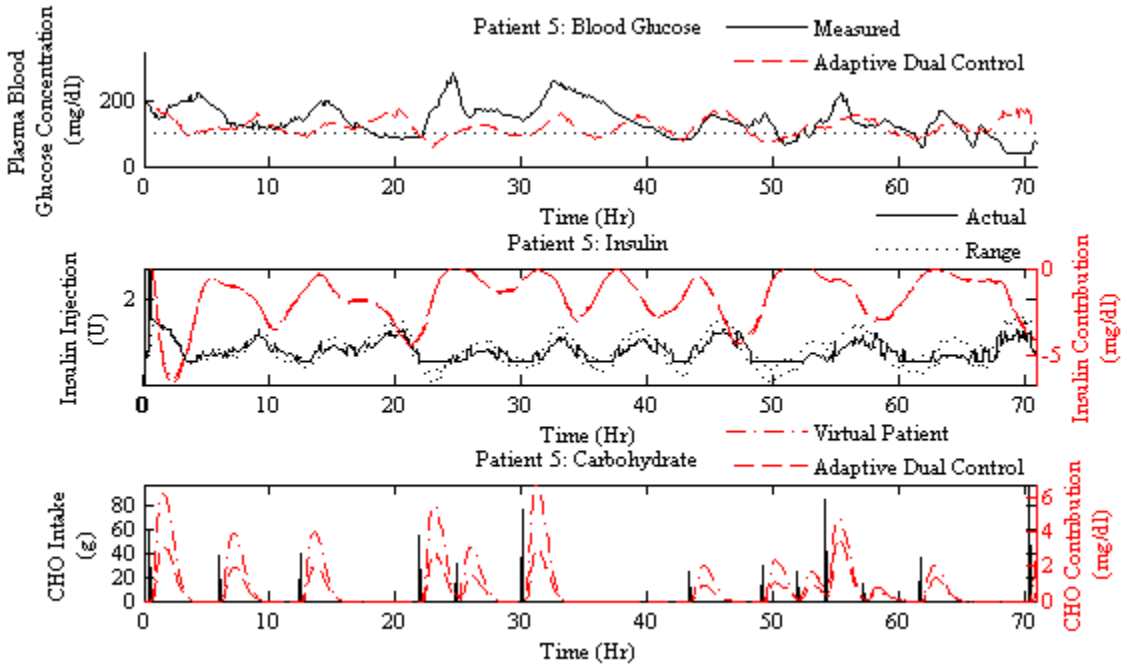

Figure 4.14: Simulated performance of adaptive dual control for patient 5.

Notice that parameter estimation for the virtual patient is conducted to implement the adaptive dual control during simulation. Comparison of the parameters of the virtual patient versus the parameter estimation under dual control provides a direct measure of estimation error to a certain extent, assuming that the virtual patient is accurate. These comparisons for patients 1, 3, 4 and 5 are given in Figure 4.15 through Figure 4.18. The initial conditions of the parameters used in parameter estimation for dual control were same as that for virtual patient (shown in Table 2.1). Figure 4.15 through Figure 4.18 show that the estimated parameters characterizing autoregression of blood glucose ($\varphi_{1\text{-}2}$) during dual control tracked fairly well. The insulin sensitivity parameters ($\beta_{1\text{-}6}$) did not track well. However the contribution tracked almost perfectly, as is subplot 2 above). Neither the carbohydrate parameters ($\gamma_{1\text{-}6}$) nor their accumulated contribution towards blood glucose tracked particularly well.

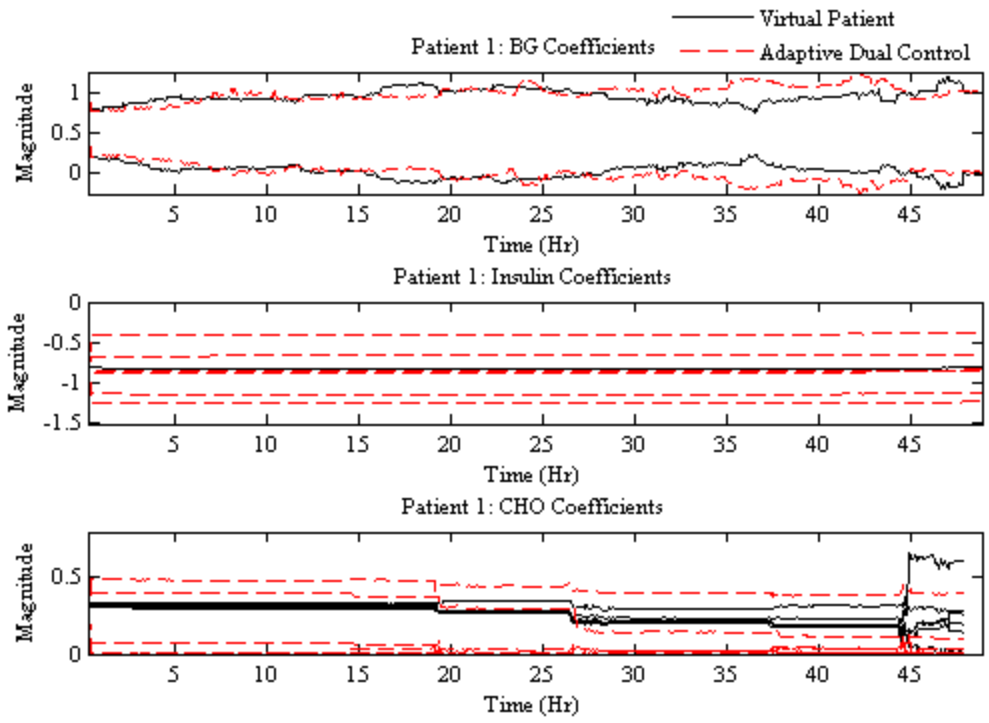

Figure 4.15: Parameter estimates for patient 1. Black solid lines represent the time-varying parameters of the virtual patient and red dashed lines represent parameters estimated during control.

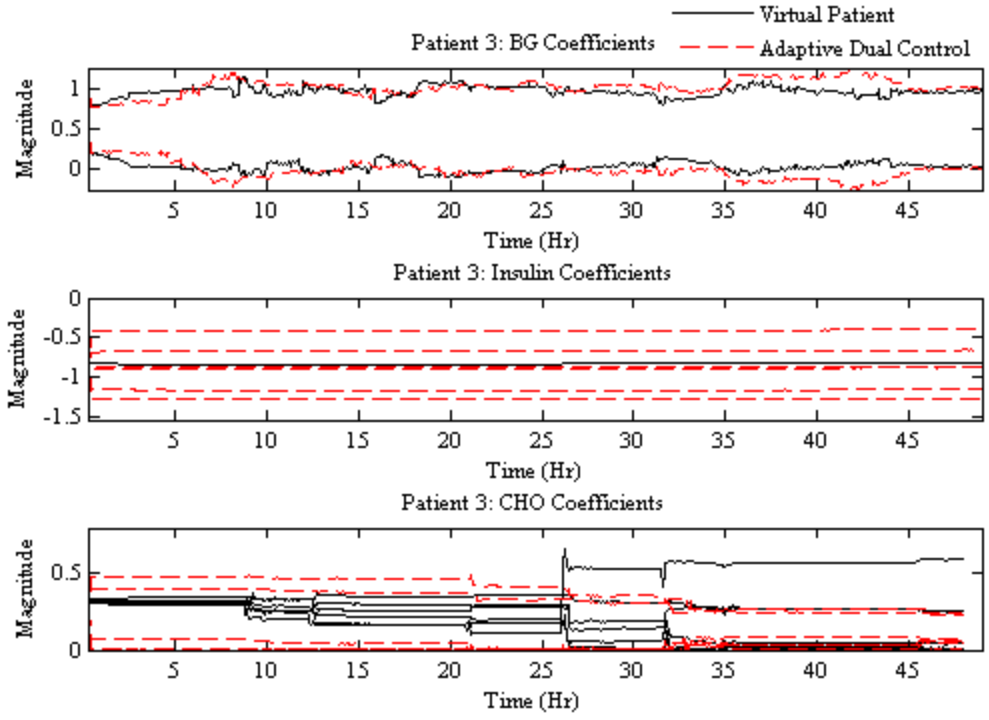

Figure 4.16: Parameter estimates for patient 3.

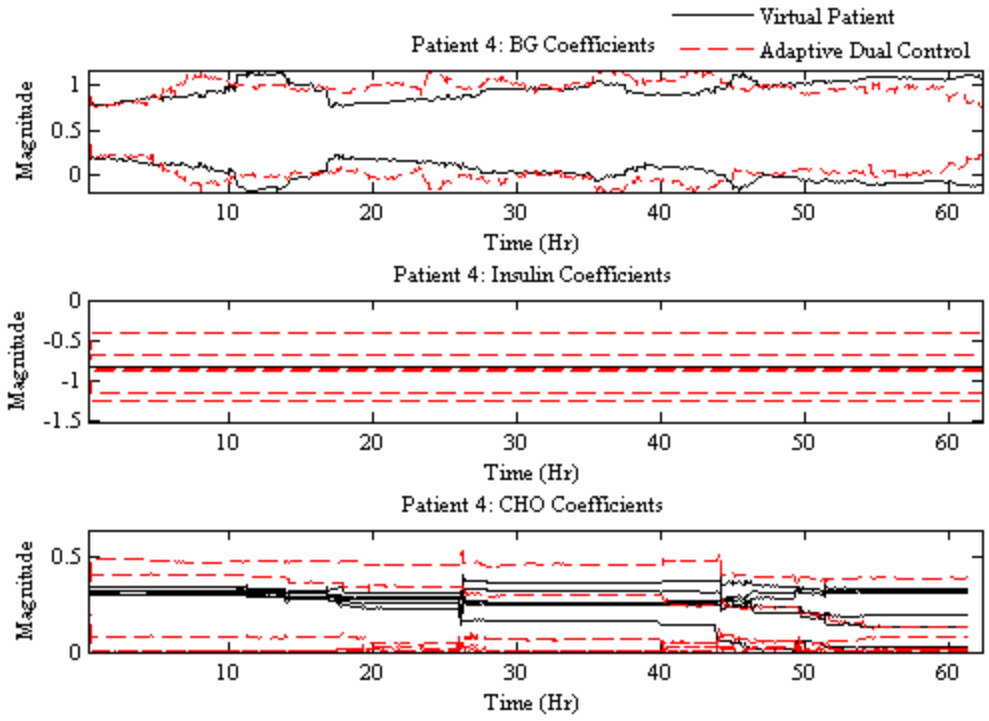

Figure 4.17: Parameter estimates for patient 4.

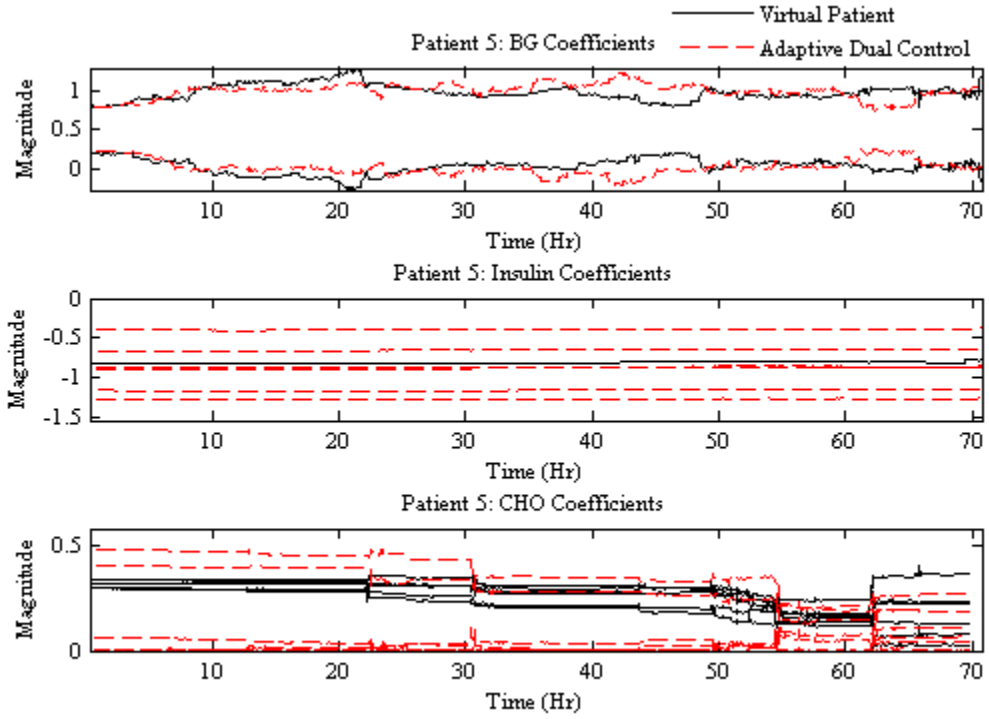

Figure 4.18: Parameter estimates for patient 5.

Presented next, is a comparison of the performance of the adaptive dual control versus the clinical treatment in terms of several community-adopted statistics: mean of blood glucose concentration, M_{80}, M_{120}, J, and the number of hypoglycemic events. Even with the small sample size, the statistics of mean blood glucose, M_{80}, M_{120}, and J, from the dual controller, were all significantly lower when compared to those calculated from the clinical measurements. In the computation of the statistics, the significance level α was 0.1, confidence level c was 0.9, in two-tailed Student's t-tests. Table 4.3 summarizes performance statistics for the clinical treatment and Table 4.4 summarizes performance statistics of the adaptive dual control algorithm. It is noted that when compared to the clinical measurements the total insulin delivery (ID) for each patient is not significantly different at the above specified confidence levels. It is also noted that under adaptive dual control there are a lower number of hypoglycemic events for patients 1 and 3. From Table 4.3, it is interesting to see that the statistics for patient 2 are, for the most part, on the high end compared to the other patients; this might be related to the instability of the adaptive dual controller.

Patient No.	Treatment Method	Mean BG (mg/dl)	Total ID (U)	n_{Hypo}*	M_{80}	M_{120}	MAGE	J
1	Clinical	149.0	110.1	3.0	474.0	202.0	128.0	45.0
2	Clinical	147.0	358.8	2.0	569.0	247.0	182.0	52.0
3	Clinical	112.0	79.4	6.0	348.0	365.0	180.0	33.0
4	Clinical	156.0	439.2	2.0	443.0	130.0	144.0	42.0
5	Clinical	141.0	256.5	1.0	333.0	114.0	127.0	36.0
Mean	(Across Patients)	141.0	248.8	2.8	433.4	211.6	152.2	41.6
Std	(Across Patients)	17.1	155.2	1.9	96.8	101.3	27.2	7.5

Table 4.3: Summary of performance statistics of clinical treatment during observation. *n_{Hypo} is the number of hypoglycemic episodes under 60 mg/dl. Total ID is the total insulin delivery during observation. Note that statistics for patient 2 are, for the most part, on the high end compared to the other patients; this might be related to the instability of the adaptive dual controller.

Patient No.	Treatment Method	Mean BG (mg/dl)	Total ID (U)	n_{Hypo}	M_{80}	M_{120}	MAGE	J
1	DC	107.4	131.9	1.0	76.7	53.5	66.5	18.2
3	DC	102.8	126.2	2.0	95.7	86.5	62.9	19.1
4	DC	100.5	109.7	2.0	48.4	62.1	49.0	15.3
5	DC	120.4	288.6	1.0	113.4	21.4	73.5	21.2
Mean	(Across Patients)	107.9	164.4	1.3	84.8	53.5	62.2	18.5
Std	(Across Patients)	8.6	83.9	0.5	30.9	26.6	12.7	2.6

Table 4.4: Summary of performance statistics of closed-loop dual control.

Chapter 5: Conclusion and Future Work

It has been shown that the dual control algorithm may be an appropriate method of connecting a blood glucose monitor to an insulin pump in the formation of an artificial pancreas (AP). Though yielding promising results, this study has certain restrictions. The first and possibly the biggest issue is the validity of the virtual patient models used in the simulation. There are two methods which are suggested in overcoming this uncertainty: build (or otherwise interface with) an FDA approved model and implement the adaptive dual control algorithms on it (another *in silico* experiment), or apply the algorithms in real-time during a supervised clinical experiment. Continuing in both directions is preferred. There were several secondary sources of potential uncertainty in this work. They include: measurement error (both real and simulated) and the accuracy of the FIR function used to characterize subcutaneous insulin and gastric absorption.

Going forward, it is recommended that the adaptive dual control methods used in this thesis be implemented on another (or several) numerical GRS model(s) prior to clinical experimentation. These other simulations will boost confidence in the methods described within this thesis especially if implemented successfully on an FDA approved GRS model. These experiments are recommended due to their low cost and lack of health risk. After these simulations, the next step would be to either test the system in real-time in a supervised clinical setting or to continue improving these methods in a virtual environment by re-running *in silico* experiments.

References

1. Ahlborg, G., Felig, P., Hagenfeldt, L., Hendler, R., Wahren, J. (1974). Substrate turnover during prolonged exercise in man: splanchnic and leg metabolism of glucose, free fatty acids, and amino acids. *Journal of Clinical Investigation*, 53, 1080-1090.
2. Al-Akwaa, F. (2008). The dynamic of glucose-insulin endocrine metabolic regulatory system: a system dynamics approach. Saarbrucken, Germany. VDM Verlag Dr. Muller Aktiengesellshaft & Co.
3. Albisser, A., Leibel, B., Ewart, T., Davidovac, Z., Botz, C., Zingg, W. (1974). An artificial endocrine pancreas. *Diabetes*, 23, 389–396.
4. Albisser, A., Leibel, B., Ewart, T., Davidovac, Z., Botz, C., Zingg, W., Schipper, H., Gander, R. (1974). Clinical control of diabetes by the artificial pancreas. *Diabetes*, 23, 397–404.
5. Bamieh, B., Giarre, L. (2002). Identification of linear parameter varying models. *International Journal of Robust and Nonlinear Control*, 12, 841-853.
6. Bar-Shalom, Y., Li, X., Kirubarajan, T. (2001). Estimation with Applications to Tracking and Navigation. John Wiley & Sons Inc.
7. Berger, M., Rodbard, D. (1989). Computer-simulation of plasma-insulin and glucose dynamics after subcutaneous insulin injection. *Diabetes Care*, 12, 725–736.
8. Bergman, R., Bucolo R. (1974). Interaction of insulin and glucose in the control of hepatic glucose balance. *American Journal of Physiology*, 227, 1314-1322.

9. Bergman, R., Ider, Z., Bowden, C., Cobelli, C., (1979). Quantitative estimation of insulin sensitivity. *American Journal of Physiology*, 236, 667-676.
10. Bergman, R., Phillips L., Cobelli, C. (1981). Physiologic evaluation of factors controlling glucose tolerance in man: measurement of insulin sensitivity and beta cell glucose from the response to intravenous glucose. *Journal of Clinical Investigation*, 68, 1456-1467.
11. Botz, C. (1976). An improved control algorithm for an artificial beta-cell. *IEEE Transactions in Biomedical Engineering*, 23, 252–255.
12. Breton, M., (2008). Physical activity: the major unaccounted impediment to closed loop control. *Journal of Diabetes Science and Technology*, 2(1), 169-174.
13. Canonico, V., Fabietti, P., Benedetti, M., Federici, M., Sarti, E., (2006). Virtual type 1 diabetic patient for feedback control systems. *Diabetes Research and Clinical Practice*, 74, 187-190.
14. Canonico, V., Federici, M., Ferolla, P., Calleno, R., Akwe J., Timi, A., Chassin, L., Wilinska, M., Vering, T., Hovorka, R., Benedetti, M. (2002). Evaluation of a feedback model based on simulated interstitial glucose for continuous insulin infusion. *Diabetologia*, 45, A322, #995.
15. Carson, E., and Cramp, D. (1976). A systems model of glucose control. *Journal of Biomedical Computing*, 7, 21-34.
16. CDC. (2007). Gestational Diabetes Fact Sheet. *Centers for Disease Control and Prevention.* <http://www.cdc.gov/diabetes/pubs/pdf/gestationalDiabetes.pdf>. Accessed Jan 11, 2011.

17. CDC. (2007). National Diabetes Fact Sheet. *Centers for Disease Control and Prevention*, 2007. <http://www.cdc.gov/diabetes/pubs/pdf/ndfs_2007.pdf>. Accessed Jan 11, 2011.
18. Clarke, W., Cox, D., Gonderfrederick, L., Carter, W., Pohl, S. (1987). Evaluating clinical accuracy of systems for self-monitoring of blood glucose. *Diabetes Care*, 10, 622–628.
19. Cobelli, C. (1984). Modelling and identification of endocrine-metabolic systems: theoretical aspects and their importance in practice. *Mathematical Biosciences*, 72, 291–235.
20. Cobelli, C., Caumo, A., Omenetto, M. (1999). Minimal model S_G overestimation and S_I underestimation: improved accuracy by a Bayesian two-compartment model. *American Journal of Physiology*. 277(3 Pt 1), E481-8.
21. Cobelli, C., Federspil, G., Pacini, G., Salvan, A., Scandellari, C., (1982). An integrated mathematical model of the dynamics of blood glucose and its hormonal control. *Mathematical Bioscience*, 58, 27-60.
22. Cobelli, C., Pacini, G., Toffolo, G., Saccà, L. (1986). Estimation of insulin sensitivity and glucose clearance from minimal model: new insights from labeled IVGTT. *American Journal of Physiology*, 250(5 Pt 1), E591-598.
23. Cobelli C., Toffolo, G., Ferrannini, E. (1984). A model of glucose kinetics and their control by insulin: compartmental and non-compartmental approaches. *Mathematical Biosciences*, 72, 291–235.
24. Cox, D., Gonder-Frederick, L., Kovatchev, B., Julian, D., Clarke, W. (1997). Understanding error grid analysis. *Diabetes Care*, 20, 911–912.

25. Cryer, P. (2002). Hypoglycemia: the limiting factor in the glycemic management of type I and type II diabetes. *Diabetologia*, 45(7), 937-48.
26. Cypress, M. (2005). Staying on target: your insulin adjustment workbook. Becton, Dickinson and Co. Albuquerque, NM. http://www.bd.com/us/diabetes/download/insulin_adjustment_workbook_complete.pdf, accessed May 27, 2011.
27. DexCom. <http://www.dexcom.com/sites/all/themes/dexcom/node-files/SEVEN_Plus_Users_Guide.pdf>, Accessed May 27, 2011. Published 2010.
28. Diabetes Research in Children Network (DirectNet) Study Group. (2004). Accuracy of the GlucoWatch G2 Biographer and the continuous glucose monitoring system during hypoglycemia: experience of the Diabetes Research in Children Network. *Diabetes Care*, 27, 722–726.
29. Docherty, P., Chase, J., Lotz, T., Hann, C., Shaw, G., Berkeley, J., Mann, J., McAuley, K. (2009). DISTq: an iterative analysis of glucose data for low-cost, real-time, and accurate estimation of insulin sensitivity. *The Open Medical Informatics Journal*, 3, 65-76.
30. Expert Committee on the Diagnosis and Classification of Diabetes Mellitus. (1997). Report of the Expert Committee on the Diagnosis and Classification of Diabetes Mellitus. *Diabetes Care*, 20(7), 1183-1197.
31. Expert Committee on the Diagnosis and Classification of Diabetes Mellitus. (2003). Follow-up report of the Expert Committee on the Diagnosis of Diabetes Mellitus. *Diabetes Care*, 26(11), 3160-3167.

32. Food and Drug Administration. <http://www.fda.gov/MedicalDevices/ProductsandMedicalProcedures/DeviceApprovalsandClearances/Recently-ApprovedDevices/ucm074293.htm>, Accessed May 18, 2011.
33. Food and Drug Administration. <http://www.fda.gov/medicaldevices/productsandmedicalprocedures/deviceapprovalsandclearances/recently-approveddevices/ucm083294.htm>. Accessed May 18, 2011.
34. Filatov, N., Unbehauen, H., (2004). Adaptive Dual Control. Springer-Verlag.
35. Foster, R., (1970). The dynamics of blood-sugar regulation. Master's Thesis, Massachusetts Institute of Technology.
36. Goodyear, L., Hirshman, M., Horton, E., (1991). Exercise-induced translocation of skeletal muscle glucose transporters. *American Journal Physiology*, 261(6 Pt 1), E795-799.
37. Hashiguchi, Y., Sakakida, M., Nishida, K., Uemura, T., Kajiwara, K., Shichiri, M. (1994). Development of a miniaturized glucose monitoring system by combining a needle-type glucose sensor with microdialysis sampling method: long-term subcutaneous tissue glucose monitoring in ambulatory diabetic patients. *Diabetes Care*, 17, 387–396.
38. Henriksen, E., (2002). Exercise effects of muscle insulin signaling and action invited review: effects of acute exercise and exercise training. *Journal of Applied Physiology*, 93, 788-796.
39. Hipszer, B., (2001). A type-1 diabetic model. Masters Thesis, Drexel University.

40. Holzinger, U., Miehsler, W., Warszawska, J., Herkner, H., Kitzberger, R., Madl, C., Wewalka, M., (2010). Real-time continuous glucose monitoring in critically ill patients: a prospective randomized trial. *Diabetes Care*, 33(3), 467-472.
41. Hovorka, R. (2005). Continuous glucose monitoring and closed-loop systems. *Diabetic Medicine*, 23, 1-12.
42. Hovorka, R. (2008). The future of continuous glucose monitoring: closed loop. *Current Diabetes Reviews*, 4(3), 269-279.
43. Hovorka, R., Allen, J., Elleri, D., Chassin, L., Harris, J., Xing, D., Kollman, C., Hovorka, T., Larson, A., Nodale, M., Palma, A., Wilinska, M., Acerini, C., Dunger, D., (2010). Manual closed-loop insulin delivery in children and adolescents with type 1 diabetes: a phase 2 randomized crossover trial. *The Lancet*, 375, 743-751.
44. Hovorka, R., Canonico, V., Chassin, L., Haueter, U., Massi-Benedetti, M., Federici, M., Piber, T., Schaller, H., Schaupp, L., Vering, T., Wilinska, M., (2004). Nonlinear model predictive control of glucose concentration in subjects with type 1 diabetes. *Physiological Measurement*, 25, 905-920.
45. Hovorka, R., Shojaee-Moradie, F., Carroll, P., Chassin, L., Gowrie, I., Jackson, N., Tudor, R., Umpleby, A., Jones, R., (2002). Partitioning glucose distribution/transport, disposal, and endogenous production during IVGTT. *American Journal of Physiology: Endocrinology and Metabolism*, 282, E992-E1007.
46. Hovorka, R., Wilinska, M., Chassin, L., Dunger, D., (). Roadmap to the artificial pancreas. *Diabetes Research and Clinical Practice*, 74, 178-182.

47. Jamurtas, A., Theocharis, V., Koukoulis, G., Stakias, N., Fatouros, I., Kouretas, D., Koutedakis, Y., (2006). The effects of acute exercise on serum adiponectin and resistin levels and their relation to insulin sensitivity in overweight males. *European Journal of Applied Physiology*, 97, 122-126.
48. Kadish A., (1963). Automation control of blood sugar: a servomechanism for glucose monitoring and control. *Transactions of the American Society for Artificial Internal Organs*, 9, 363–367.
49. Kan, S., Onodera, H., Furuntani, E., Aung, T., Araki, M., Nishimura, H., Maetani, S., Imamura, M. (2000). Novel control system for blood glucose using a model predictive method. *Journal of the American Society of Artificial Internal Organs*, 657-662.
50. Kirchsteiger, H., Re, L., Renard, E., Mayrhofer, M., (2009). Robustness properties of optimal insulin bolus administrations for type 1 diabetes. *American Control Conference*, 2284-2289.
51. Kraegen, E., Campbell, L., Chia, Y., Meler, H., Lazarus, L. (1977). Control of blood glucose in diabetics using an artificial pancreas. *Australian & New Zealand Journal of Medicine*, 7, 280–286.
52. Leblanc, H., Chauvet, D., Lombrail, P., Robert, J. (1986). Glycemic control with closed-loop intraperitoneal insulin in type 1 diabetes. *Diabetes Care*, 9, 124–128.
53. Lee, R., Nieman, D. (2007). Nutritional assessment. 4th ed. Boston: McGraw-Hill.

54. Lehmann, E., and Deutsch, T., (1992). Physiological model of glucose-insulin interaction in type-1 diabetes mellitus. *Journal of Biomedical Engineering*, 14(3), 235-242.

55. Li, J., (2004). The dynamics of glucose-insulin endocrine metabolic regulatory system. PhD Thesis, Arizona State University.

56. Magni, L., Raimondo, D., Man, C., Breton, M., Patek, S., Nicolao, G., Cobelli, C., Kovatchev, B. (2008). Evaluating the efficacy of closed-loop glucose regulation via control-varibility grid analysis. *Journal of Diabetes Science and Technology*, 2(4), 630-635.

57. Makroglou, A., Li, J., Kuang, Y., (2006). Mathematical models and software tools for the glucose-insulin regulatory system and diabetes: an overview. *Applied Numerical Mathematics*, 56, 559-573.

58. Man, C., Camilleri, M., Cobelli, C. (2006). A system model of oral glucose absorption: validation on gold standard data. *IEEE Transactions. Biomedical Engineering*, 53(12), 2472–2478.

59. Man, C., Rizza, R., Cobelli, C. (2007). Meal simulation model of the glucose-insulin system. *IEEE Transactions on Biomedical Engineering*, 54(10), 1740-1749.

60. Marchetti, G., Barolo, M., Jovanovic, L., Zisser, H. Seborg, D., (2008). An improved PID switching control strategy for type 1 diabetes. *IEEE Transactions on Biomedical Engineering*, 55(3), 857-865.

61. Marliss, E., Murray, F., Stokes, E., Zinman, B., Nakhooda, A., Denoga, A., Leibel, B., Albisser, A. (1977). Normalization of glycemia in diabetics during

meals with insulin and glucagon delivery by the artificial pancreas. *Diabetes*, 26, 663–672.

62. McGowan, K., Thomas, W., Moran, A. (2002). Spurious reporting of nocturnal hypoglycemia by CGMS in patients with tightly controlled type I diabetes. *Diabetes Care*, 25, 1499–1503.
63. Metzger, M., Leibowitz, G., Wainstein, J., Glaser, B., Raz, I. (2002). Reproducibility of glucose measurements using the glucose sensor. *Diabetes Care*, 2002; 25: 1185–1191.
64. MiniMed Medtronic. <http://www.minimed.com/swf/guardian/pdf/sensor_accuracy.pdf>. Accessed May 18, 2011.
65. Molenaar, P., Wang, Q., Freeman, K., Zhou, J., Gold, C., Rovine, M., Ulbrecht, J. (2011). State-space modeling of continuously monitored blood glucose time series of type 1 diabetic patients: a new inductive approach to prediction and dynamic regression on insulin dose and meal intake. Submitted to *Diabetes Care*.
66. National Diabetes Data Group. (1979). Classification and diagnosis of diabetes mellitus and other categories of glucose intolerance. *Diabetes*, 28, 1039-57.
67. Olansky, L., Kennedy, L., (2010). Finger-stick glucose monitoring: issues of accuracy and specificity. *Diabetes Care*, 33, 948-949.
68. Parker, R., Doyle, F., Peppas, N., (1999). A model-based algorithm for blood glucose control in type 1 diabetic patients. *IEEE Transactions on Biomedical Engineering*, 46(2), 148-57.

69. Pickup, J., Keen, H. (2002). Continuous subcutaneous insulin infusion at 25 years: evidence base for the expanding use of the insulin pump therapy in type 1 diabetes. *Diabetes Care*, 25(3), 593-598.

70. Pickup, J., Keen, H., Parsons, J., Alberti, K. (1978). Continuous subcutaneous insulin infusion: an approach to achieving normoglycaemia. *British Medical Journal*, 1, 204–207.

71. Plank, J., Wutte, A., Brunner, G., Siebenhofer, A., Semlitsch, B., Sommer, R. Brunner, G., Hirschberger, S., Siebenhofer, A., Pieber, T. (2002). A direct comparison of insulin aspart and insulin lispro in patients with type 1 diabetes. *Diabetes Care*, 25, 2053–2057.

72. Rebrin, K., Steil, G., van Antwerp, W., Mastrototaro, J. (1999). Subcutaneous glucose predicts plasma glucose independent of insulin: implications for continuous monitoring. *American Journal of Physiology: Endocrinology and Metabolism*, 277, E561–E571.

73. Regitting, W., Trajanoski, Z., Leis, H., Ellmerer, M., Wutte, A., Sendlhofer, G., Schaupp, L., Brunner, G., Wach, P., Pieber, T. (1999). Plasma and interstitial glucose dynamics after intravenous glucose injection: evaluation of the single-compartment glucose distribution assumption in the minimal models. *Diabetes*, 48, 1070–1081.

74. Renard, E. (2002). Implantable closed-loop glucose-sensing and insulin delivery: the future for insulin pump therapy. *Current Opinions in Pharmacology*, 2(6), 708-716.

75. Renard, E., (2008). Implantable continuous glucose sensors. *Current Diabetes Reviews*, 4, 169-174.

76. Renard, E., Chevassus, H., Place, J., Palerm, C., Cantwell, M. (2010). Closed loop insulin delivery using a subcutaneous glucose sensor and intraperitoneal insulin delivery. *Diabetes Care*, 33, 121-127.

77. Renard, E., Costalat, G., Chevassus, H., Bringer, J. (2006). Closed loop insulin delivery using implanted insulin pumps and sensors in type 1 diabetic patients. Diabetes Research and Clinical Practice, 74 Supp. 2, S173-S177.

78. Roy, A., (2008). Dynamic modeling of free fatty acid, glucose, and insulin during rest and exercise in insulin dependent diabetes mellitus patients. PhD Thesis, University of Pittsburgh, 2008.

79. K. Ruder. (2007). A Week of Continuous Monitoring. *Diabetes Forecast*; 60, 10.

80. Schlichtkrull, J., Munck, O., Jersild, M. (1965). The M-value, an index of blood sugar control in diabetics. *Acta Medica Scandinavica*, 177, 95–102.

81. Service, F., Molnar, G., Rosevear, J., Ackerman, E., Gatewood, L., Taylor, W. (1970). Mean amplitude of glycemic excursions, a measure of diabetic instability. *Diabetes*, 19, 644–655.

82. Sherwin, R., Kramer, K., Tobin, J., Insel, P., Liljenquist, J., Berman, M., Andres, R., (1974). A model of the kinetics of insulin in man. *Journal of Clinical Investigation*, 53, 1481-1492.

83. Shichiri, M., Kawamori, R., Goriya, Y., Yamasaki, Y., Nomura, M., Hakui, N., Abe, H. (1983). Glycemic control in pancreatectomized dogs with a wearable artificial endocrine pancreas. *Diabetologia*, 24, 179-184.

84. Shichiri, M., Kawamori, R., Hakui, N., Yamasaki, Y., Abe, H. (1984). Closed-loop glycemic control with a wearable artificial endocrine pancreas: variations in daily insulin requirements to glycemic response. *Diabetes*, 33, 1200-1202.

85. Steil, G., Panteleon, A., Rebrin, K., (2004). Closed-loop insulin delivery: the path to physiological glucose control. *Advanced Drug Delivery Reviews*, 56, 125-144.

86. Steil, G., Rebrin, K., Darwin, C., Hariri, F., Saad, M. (2006). Feasibility of automating insulin delivery for the treatment of type 1 diabetes. *Diabetes*, 55(12), 3344-3350.

87. Steil, G., Rebrin, K., Mastrototaro, J., (2006). Metabolic modeling and the closed-loop insulin delivery problem. *Diabetes Research and Clinical Practice*, 74, 183-186.

88. Stout, P., Racchini, J., Hilgers, M., Noujaim, S., (2006). Continuous glucose monitoring: key challenges to replacing epsiodic SMBG. *Diabetes Research and Clinical Practice*, 74, 97-100.

89. Sturis, J., Polonsky, K., Moseklide, E. van Cauter, E., (1991). Computer model for mechanisms underlying ultradian oscillations of insulin and glucose. *American Journal of Physiology: Modeling Methodology Forum*, 193, E801-E809.

90. Thorell, A., Hirshman, M., Nygren, J., Jorfeldt, L., Wojtaszewski, J., Dufresne, S., Horton, E., Ljungqvist, O., Goodyear, L. (1999). Exercise and insulin cause GLUT-4 translocation in human skeletal muscle. *American Journal of Physiology*, 277(4 Pt 1), E733-E741.

91. Waldhäusl, W., Bratusch-Marrain, P., Komjati, M., Breitenecker, F., Troch, I. (1992). Blood glucose response to stress hormone exposure in healthy man and

insulin dependent diabetic patients: prediction by computer modeling. *IEEE Transactions on Biomedical Engineering*, 39(8), 779-790.

92. Weinstein, R., Bugler, J., Schwartz, S., Peyser, T., Brazg, R., McGarraugh, G. (2007). Accuracy of the 5-Day FreeStyle Navigator continuous glucose monitoring system. *Diabetes Care*, 30, 1125-1130.
93. Weller, C., Linder, M., Macaulay, A., Ferrari, A., Kessler, G. (1960). Continuous *in vivo* determination of blood glucose in human subjects. *Annals of the NY Academy of Sciences*, 87, 658–668.
94. Wojcicki, J., (1995). "J"-index. a new proposition of the assessment of current glucose control in diabetic patients. *Hormone and Metabolic Research*, 27, 41–42.
95. Zhou, J., Wang, Q., Molenaar, P., Ulbrecht, J., Gold, C., Rovine, M., (2010). Receding horizon control of type 1 diabetes based on a data-driven linear time-varying state-space model. *Proceedings of the American Control Conference*, Baltimore, MD. June 2010, 568-573.